Supporting Information

Organic Contaminant Abatement in Reclaimed Water by UV/H_2O_2 and a Combined Process consisting of O_3/H_2O_2 followed by UV/H_2O_2: Prediction of abatement efficiency, energy consumption, and by-product formation

YUNHO LEE[1,2]*, DANIEL GERRITY[3,4,5]**, MINJU LEE[2,6], SUJANIE GAMAGE[5], ALEKSEY PISARENKO[4,5], REBECCA A. TRENHOLM[5], SILVIO CANONICA[2], SHANE A. SNYDER[7], AND URS VON GUNTEN[2,6]

[1]*School of Environmental Science and Engineering, Gwangju Institute of Science and Technology, 123, Oryong-dong, Buk-gu, Gwangju 500-712, Korea*

[2]*Eawag, Swiss Federal Institute of Aquatic Science and Technology, Ueberlandstrasse 133, P.O. Box 611, 8600 Duebendorf, Switzerland*

[3]*Department of Civil and Environmental Engineering, University of Nevada, Las Vegas, Box 454015, 4505 S. Maryland Parkway, Las Vegas, NV 89154-4015, United States*

[4]*Trussell Technologies, Inc., 6540 Lusk Blvd., Suite C274, San Diego, CA 92121, United States*

[5]*Applied Research and Development Center, Southern Nevada Water Authority, P.O. Box 99954, Las Vegas, NV 89193-9954, United States*

[6]*School of Architecture, Civil, and Environmental Engineering (ENAC), École Polytechnique Fédérale de Lausanne, CH-1015, Lausanne, Switzerland*

[7]*Department of Chemical and Environmental Engineering, University of Arizona, 1133 E. James E. Rogers Way, Harshbarger 108, Tucson, AZ 85721-0011, United States*

*Corresponding author. Mailing address: School of Environmental Science and Engineering, Gwangju Institute of Science and Technology, 123, Oryong-dong, Buk-gu, Gwangju 500-712, Korea. Phone: (82) 62 715 2468. Fax: (82) 62 715 2434. Email: yhlee42@gist.ac.kr.

**Corresponding author. Mailing address: Department of Civil and Environmental Engineering, University of Nevada, Las Vegas, Box 454015, 4505 S. Maryland Parkway, Las Vegas, NV 89154-4015, United States. Phone: (702) 895-3955. Fax: (702) 895-3936. Email: Daniel.Gerrity@unlv.edu.

Supplementary Information

54 pages, 8 texts, 4 tables, and 12 figures are available for further information addressing materials, experimental procedures and additional data.

SI-Text-1. Standards and reagents

All chemicals and solvents (95% purity or higher) were purchased from various commercial suppliers and used as received. Stock solutions of hydrogen peroxide (10 mM) were prepared by diluting 30% H_2O_2 solution from Sigma-Aldrich. H_2O_2 stock solutions were standardized spectrophotometrically based on the molar absorption coefficients: $\varepsilon = 40\ M^{-1}\ cm^{-1}$ at 240 nm.[1] A stock solution of a micropollutant mixture (atenolol, atrazine, bisphenol A, carbamazepine, N,N-diethyl-meta-toluamide (DEET), diclofenac, gemfibrozil, ibuprofen, meprobamate, naproxen, phenytoin, primidone, sulfamethoxazole, triclosan, and trimethoprim) was prepared in deionized water at a concentration of ~2 mg/L for each micropollutant. The stock solution was stored in 4°C and all micropollutants in the stock solution were stable during the experimental period (a few months).

SI-Text-2. Analytical methods

Micropollutant analyses. The selected 16 micropollutants except NDMA were analyzed using a Symbiosis (Spark Holland, Emmen, the Netherlands) automated on-line solid phase extractor and a 4000 QTRAP triple quadrupole-linear ion trap hybrid mass spectrometer (ABSCIEX, Foster City, CA, USA). The method described below is adapted from Snyder et al.[2] or Lee et al., 2013.[3] Online

SPE-LC-MS/MS was accomplished with a Symbiosis™ Pharma (Spark Holland, Emmen, the Netherlands) system in XLC mode using Analyst® 1.4.2 (Applied Biosystems, Foster City, CA). Samples were collected in 40-mL amber glass vials with quenching agents and preservatives as described previously. If analysis was not performed immediately following each experiment, samples were refrigerated at 4°C and extracted within 14 days of collection. Prior to analysis, 10 mL of sample was measured in a volumetric flask and spiked with isotopically-labeled standards at 100 ng/L. This provided sufficient sample volume for replicates, matrix spikes, and dilutions, if necessary. A 1.5-mL aliquot of each sample was transferred into a 2-mL autosampler vial, although only 1.0 mL was used for extractions. Extractions were performed using Waters Oasis HLB Prospekt cartridges (30 mm, 2.5 mg, 10 x 1 mm, 96 tray) (Milford, MA). Prior to sample loading, each cartridge was sequentially conditioned with 1 mL of dichloromethane, methyl tert-butyl ether (MTBE), methanol, and reagent water (Milli-Q). Samples were loaded onto the SPE cartridges at 1 mL/min after which the cartridges were washed with 1 mL of reagent water. After sample loading, the analytes were eluted from the SPE cartridge to the LC column with 200 mL methanol, using the LC peak focusing mode. A 5-mM ammonium acetate solution and methanol gradient was used for LC mobile phases with a flow rate of 800 mL/min. Analytes were separated using a 150 x 4.6-mm Luna C18(2) column with a 5-μm particle size (Phenomenex, Torrance, CA). Method reporting limits (MRLs) were established at 3 to 5 times the method detection limits (MDLs). Although lower MRLs can be achieved with offline SPE-LC-MS/MS methods, the elevated concentrations in wastewater, particularly after spiking at 1 μg/L, were sufficient to justify the use of the online alternative. Stringent QA/QC protocols (i.e. matrix spikes, duplicate samples, field blanks, and laboratory blanks) were followed throughout the duration of the project. Based on extensive method development and past studies, the concentrations of duplicate samples rarely varied by greater than 5%.

NDMA was quantified with isotope dilution using a modified version of U.S. Environmental Protection Agency (EPA) method 521.[4,5] Automated solid phase extraction was performed using a Dionex AutoTrace workstation (Thermo Scientific, Sunnyvale, CA, USA). Samples (1000 ml) were spiked with isotopically labeled standard (NDMA-d_6) and extracted with prepacked activated coconut charcoal cartridges (Resprep™ 521, Restek, Bellefonte, PA). Extracts were concentrated to a final volume of 0.5 mL (a concentration factor of 2000). A Varian (Walnut Creek, CA) CP-3800 Gas Chromatograph with a CP-8400 autosampler was used for separation. The injector was operated

in splitless mode (injection volume of 2 μL) at 200°C. Analytes were separated on a 30 m × 0.32 mm i.d. × 1.8 μm DB 624 column (Agilent, PaloAlto, CA) using a 1.2 mL/min helium flow with an initial pressure pulse of 35 psi for 0.85 min. The temperature program was: 35 °C, hold for 1.0 min; 35–120 °C at 5 °C/min; 120–145 °C at 3 °C/min; 145–250 °C at 35 °C/min, hold for 4.64 min. A Varian 4000 ion trap mass spectrometer was used for analysis in conjunction with multiple reaction monitoring (MRM) in positive chemical ionization mode. The $^{\bullet}$OH probe compound *para*-chlorobenzoic acid (*p*CBA) was quantified with direct injection and liquid chromatography tandem mass spectrometry according to a previously published method.[6]

Bulk Organic matter analysis. For the five U.S. wastewaters, dissolved organic carbon (DOC) was analyzed by a Shimadzu (Columbia, MD) Total Organic Carbon analyzer after sample acidification to pH <3 with hydrochloric acid, and filtration with 0.45-μm membrane filters (GHP Acrodisc, Pall Life Sciences). For the other wastewaters (CH and AUS), DOC was analyzed by LC-OCD instrument.[7] Laboratory filtration was also performed prior to the UV-Vis analyses. Absorption spectra were measured using a PerkinElmer (Waltham, MA) Lambda 45 UV-Vis Spectrometer, consistent with Standard Method 5910 B. This instrument was also used to determine the decadic molar extinction coefficients for the various micropollutants, which were spiked at 10 mg L^{-1} (34-52 μM) in nanopure water. Further details of the bulk organic matter characteristics can be found elsewhere.[3,8]

SI-Text-3. Bench-scale UV and UV/H_2O_2 experiments for micropollutant abatement in wastewater effluents

For the five U.S. wastewaters, two collimated beams were constructed based on the protocols of Bolton and Linden[9] and Kuo et al.[10] The collimated beam apparatuses contained one or two 46-cm, 15-watt, low-pressure, mercury arc bulbs (Model G15T8, Ushio, Cypress, CA). The bulbs produced nearly monochromatic, germicidal light at a peak wavelength of 254 nm. The collimated beam apparatus included adjustable platforms and slow-speed stir plates to ensure proper mixing during the irradiation periods. Following a 5-min warm-up period for the UV lamp, the intensity of the UV light was measured using an IL1700 research radiometer with sensor SUD240 (International Light, Newburyport, MA). A calibration on each component, traceable to National Institute of Standards and Technology (NIST) standards, was performed by the manufacturer prior to the experiments.

Prior to the irradiation experiments, the platform was adjusted to ensure that the surface of the radiometer detector and the wastewater samples were at the same level during the calibration and irradiation phases, respectively. Experiments were performed in a 100-mL beaker with a diameter of 5.5 cm and a sample depth of 4.2 cm. The experiments were repeated in 100-mL aliquots until sufficient sample volumes had been collected for the various analytical methods. The incident UV intensities for these collimated beams were approximately 0.23 mW cm^{-2} (system A) and 0.58 mW cm^{-2} (system B). UV doses were calculated as the product of the incident UV intensity, a series of collimated beam correction factors[9,10] and exposure times. The corrections accounted for the reflection factor (RF), Petri factor (PF), divergence factor (DF), and water factor (WF) associated with each collimated beam. The WF is defined as $WF = (1 - 10^{-A254nm \times L})/(2.303 \times A_{254nm} \times L)$ in which A_{254nm} (cm^{-1}) is the absorbance of the sample water matrix for a 1-cm path length, and L (cm) is the vertical light path length. The correction parameters for system A were as follows: RF = 0.98, PF = 0.51, DF = 0.91, and WF = 0.36 – 0.59. The correction parameters for system B were as follows: RF = 0.98, PF = 0.95, DF = 0.84, and WF = 0.36 – 0.59.

For the wastewaters from CH and AUS, the UV experiments were conducted in a DEMA 125 merry-go-round photoreactor (Hans Mangels, Bornheim-Roisdorf, Germany) equipped with a low-pressure mercury lamp (model TNN 15/32, Heraeus Noblelight, Hanau, Germany) emitting nearly monochromatic light at 254 nm. The lamp was contained in a quartz cooling jacket, and the photoreactor was filled with deionized water kept at a constant temperature of 25°C. Sample solutions, typically 20 mL, were contained in quartz tubes. The average light path length (L) in the quartz tubes was calculated to be 1.2 cm and used for the WF calculation. Fluence and fluence rate values were determined by chemical actinometry at low optical density using 5 μM aqueous atrazine as an actinometer. The average UV fluence rate for the merry-go-round photoreactor was approximately 1.4 mW cm^{-2}. The RF, PF, and DF parameters in this photochemical system are assumed to be '1'. Thus, UV doses were calculated as the product of the UV fluence rate, water factor, and exposure times. The WF ranged from 0.60 to 0.87 for the five wastewater effluents from CH and AUS. Further details of the merry-go-round photoreactor system and the atrazine actinometry can be found elsewhere.[11]

UV doses for the various wastewaters ranged from 23-2679 mJ cm^{-2}, and the H_2O_2 dose for each experiment was 0 and 10 mg L^{-1} (a few experiments were performed using 5 mg L^{-1} of H_2O_2). For the micropollutant experiments, approximately 1 μg/L (3.4-5.2 nM) of each target compound listed

in Table 1 was spiked into each sample. Samples used to assess NDMA photolysis were spiked with approximately 150-300 ng/L (2.1-4.2 nM) of NDMA. Following UV irradiation, samples were preserved with 1 g L^{-1} of sodium azide, and stored at 4 °C prior to analysis.

SI-Text-4. Kinetic models for micropollutant abatement in UV and UV/H_2O_2 processes

The abatement of a micropollutant in the UV or UV/H_2O_2 process is mainly achieved by its direct UV photolysis or a combination of UV photolysis and oxidation by •OH, respectively, in which •OH is produced from H_2O_2 photolysis.[12] The micropollutant abatement rate in a batch reactor under a quasi-collimated beam system can be described by Eq. S1 for the UV process and Eq. S2 for the UV/H_2O_2 process.

$$-\frac{d[MP]}{dt} = k_{UV} \times [MP] \quad \text{(S1)}$$

$$-\frac{d[MP]}{dt} = (k_{UV} + k_{\bullet OH,MP}[\bullet OH]_{ss}) \times [MP] \quad \text{(S2)}$$

In Eq. S1, k_{UV} is the pseudo-first-order rate constant (s^{-1}) for micropollutant abatement and can be expressed as $k_{UV} = 2.303 \times \varepsilon_{MP} \times \Phi_{MP} \times E'_{p,ave}$ where ε_{MP} (m^2 mol^{-1}) and Φ_{MP} (mol $einstein^{-1}$) are the molar absorption coefficient and the phototransformation quantum yield of a micropollutant, respectively. $E'_{p,ave}$ (einstein m^{-2} s^{-1}) is the average photon fluence rate throughout the solution. It is related to E_p^0, the incident photon fluence rate at the center of the sample surface (i.e., $E_{ave}^0 = E_p^0 \times RF \times PF \times DF \times WF$ in which the correction parameters were introduced previously in SI-Text-3). In Eq. S2, $k_{\bullet OH,MP}$ is the second-order rate constant for the reaction of •OH with micropollutant, and $[\bullet OH]_{ss}$ is the steady-state •OH concentration that can be expressed as the ratio of the zero-order •OH formation rate ($v_{\bullet OH}$, M s^{-1}) over the first-order •OH consumption rate constant ($\sum_i k_{Si}[S_i]$, s^{-1}), i.e., $[\bullet OH]_{ss} = \frac{v_{\bullet OH}}{\sum_i k_{Si}[S_i]}$, M. The zero-order •OH formation rate in the UV/H_2O_2 process can be expressed as $v_{\bullet OH} = 2.303 \times \varepsilon_{H2O2} \times \Phi_{\bullet OH} \times [H_2O_2] \times E_{ave}^0$ in which ε_{H2O2} (= 1.96 m^2 mol^{-1}) is the molar absorption coefficient of H_2O_2 and $\Phi_{\bullet OH}$ (=1 mol $einstein^{-1}$) is the •OH formation quantum yield from H_2O_2 photolysis (i.e., $H_2O_2 + hv \rightarrow 2^{\bullet}OH$).[12] The first-order •OH scavenging rate constant, $\sum_i k_{Si}[S_i]$, can be calculated by summing the product of the concentration of each water matrix

component, S_i, with the corresponding second-order rate constant, k_{Si}. The complete derivation of Eq. S1 and S2 can be found elsewhere.[9,13,14]

The integration of Eqs. S1 and S2 over time and the introduction of the relationship between time and UV dose (i.e., UV dose = $H' = E'_{p,ave} \times t \times U/10$ and $U = 4.72 \times 10^5$ J einstein^{-1} at 254 nm) yield Eqs. S3 and S4, in which the logarithmic relative concentration of micropollutant is linearly related to UV dose (i.e., H′), a key controlling parameter for the UV and the UV/H_2O_2 processes.

$$-\ln\left(\frac{[MP]_t}{[MP]_0}\right) = k_{UV} \times t = \frac{2.303 \times 10}{U} \times \varepsilon_{MP} \times \Phi_{MP} \times H' = k_{UV\text{-}pred} \times H' \quad \text{(S3)}$$

$$-\ln\left(\frac{[MP]_t}{[MP]_0}\right) = (k_{UV} + k_{\bullet OH}[^{\bullet}OH]_{ss}) \times t = \frac{2.303 \times 10}{U} \times \left(\varepsilon_{MP} \times \Phi_{MP} + \frac{k_{\bullet OH,MP} \times \varepsilon_{H2O2} \times \Phi_{\bullet OH} \times [H_2O_2]}{\sum_i k_{Si}[S_i]}\right) \times H'$$

$$= (k_{UV\text{-}pred} + k'_{\bullet OH\text{-}pred}) \times H' = k_{UV/H2O2\text{-}pred} \times H' \quad \text{(S4)}$$

where, $k_{UV\text{-}pred} = \frac{10 \times k_{UV}}{E'_{p,ave} \times U} = \frac{2.303 \times 10}{U} \times \varepsilon_{MP} \times \Phi_{MP}$ (S5)

$$k'_{\bullet OH\text{-}pred} = \frac{10 \times k_{\bullet OH,MP} \times [\bullet OH]_{ss}}{E'_{p,ave} \times U} = \frac{2.303 \times 10}{U} \times \frac{k_{\bullet OH,MP} \times \varepsilon_{H2O2} \times \Phi_{\bullet OH} \times [H_2O_2]}{\sum_i k_{Si}[S_i]} \quad \text{(S6)}$$

In Eqs. S3 and S4, '10' is introduced as the fluence unit conversion factor for the use of mJ cm^{-2} instead of J m^{-2}, U is the molar photon energy at 254 nm, H′ is the average UV fluence (mJ cm^{-2}) throughout the solution, $k_{UV\text{-}pred}$ (mJ^{-1} cm^2) is the fluence-based transformation rate constant of micropollutant by UV during UV or UV/H_2O_2 treatment and $k'_{\bullet OH\text{-}pred}$ (mJ^{-1} cm^2) is the fluence-based transformation rate constant of micropollutant by •OH during UV/H_2O_2 treatment. Finally, $k_{UV/H2O2\text{-}pred}$ is the overall fluence-based transformation rate constant of a micropollutant during UV/H_2O_2 treatment (i.e., $k_{UV/H2O2\text{-}pred} = k_{UV\text{-}pred} + k'_{\bullet OH\text{-}pred}$). Further details of this 'steady-state •OH model' can be found elsewhere.[14,15]

SI-Text-5. Changes of major water matrix components during treatment and their influence on model predictions

In the model prediction of micropollutant abatement by Eqs. 2 and 3, the initial conditions for the water matrix components, such as water absorbance at 254nm (A_{254nm}) and concentrations of

DOC, carbonate species, NO_2^-, and Br^-, were kept constant for the entire duration of the UV experiments. These water matrix components might change significantly during UV/H_2O_2 treatment by the reactions with •OH (e.g., oxidative transformation or decolorization) and may affect the model predictions. Here, the changes of these water matrix components and their possible influence on the micropollutant abatement prediction are discussed.

A_{254nm}. The A_{254nm} was observed to decrease by up to 30% with an increasing UV dose of up to 1000 mJ cm^{-2} (data not shown). The A_{254nm} decrease can be attributed to the reaction of •OH with the DOM chromophores. The A_{254nm} decrease during UV alone treatment was insignificant. The water factor, i.e., $WF = (1 - 10^{-A254nm \times L})/(2.303 \times A_{254nm} \times L)$ depends on the A_{254nm} and the light path length (L). The calculations show that the WF could have increased by 4 – 15% for the wastewaters from CH and AUS (L = 1.2) and by 16 – 30% for the US wastewaters (L = light path length = 4.2 cm) for an UV dose of 1000 mJ cm^{-2}, which would increase the rate of •OH formation.

H_2O_2. The decrease of H_2O_2 during UV/H_2O_2 treatment can mainly occur by photolysis of H_2O_2 (i.e., $H_2O_2 + h\nu \rightarrow 2$•OH), and the rate can be described as Eq. S7. The reaction of H_2O_2 with •OH can be neglected in wastewater effluent matrices considering its low reaction rate ($k = 3\times10^7$ M^{-1} s^{-1}) compared to the •OH consumption rate by the matrix components. The calculation using Eq. S7 shows that the decrease of H_2O_2 is less than 10% of its initial concentration within the UV_{dose} range of 0 – 2000 mJ/cm^2. Thus, it can be assumed that the H_2O_2 concentration during UV/ H_2O_2 treatment remains practically constant in the typical UV_{dose} range.

$$-\ln\left(\frac{[H_2O_2]_t}{[H_2O_2]_0}\right) = \frac{2.303\times10}{U}\times\varepsilon_{H2O2}\times\Phi_{H2O2}\times H' \qquad \text{(S7)}$$

where, ε_{H2O2} (= 1.9 m^2 mol^{-1}) is the molar absorption coefficient of H_2O_2, and Φ_{H2O2} (= 0.5 mol $einstein^{-1}$)[12] is the quantum efficiency of H_2O_2 decomposition.

DOM and carbonate species. The concentration of DOC and carbonate species remains almost constant during typical UV/H_2O_2 treatment conditions. In addition, the degradation products of DOM have been shown to have similar reactivity to •OH compared to the original DOM.[16]

Br^-. The concentration of Br^- is expected to vary little during UV/H_2O_2 treatment due to the relatively slow net reaction of Br^- with •OH. Br^- reacts very rapidly with •OH, but it is a pre-equilibrium process (Br^- + •OH $\rightleftharpoons$ $BrOH^-$•, $BrOH^-$• $\rightarrow$ Br• + OH^-) and the apparent second-order rate constant for the reaction of Br^- with •OH is 1.1×10^9 M^{-1} s^{-1}.[17] Br• can be reduced to Br^- by its reaction dissolved organic matter (Br• + DOM $\rightarrow$ Br^- + DOM•$^+$, k = 10^9 M^{-1} s^{-1}).[18] In

addition, HOBr, the key oxidation intermediate of Br^- oxidation, can be rapidly reduced to Br^- by hydrogen peroxide (i.e., $HOBr + HO_2^- \rightarrow Br^- + H_2O$, $k = 7.6\times10^8\ M^{-1}\ s^{-1}$).[17] Finally, the contribution of Br^- to the overall •OH consumption rate in the studied wastewater effluents was less than 10%.

NO_2^-. The concentration of NO_2^- can decrease by its rapid reaction with •OH ($NO_2^- + \bullet OH \rightarrow NO_2\bullet + OH^-$, $k_{\bullet OH,NO2-} = 1\times10^{10}\ M^{-1}\ s^{-1}$) or UV photolysis ($NO_2^- + h\nu \rightarrow [NO_2^-]^* + H^+ \rightarrow NO\bullet + \bullet OH$), or increase by the photolysis of NO_3^- ($NO_3^- + h\nu \rightarrow \rightarrow NO_2^- + 1/2O_2$).[19] Nevertheless, the calculations show that the oxidation of NO_2^- by •OH is dominant over the two other pathways in the studied wastewater effluent matrices (see below). For higher NO_2^- and lower DOC concentration, the decrease of NO_2^- became more pronounced due to the increasing level of NO_2^- oxidation by •OH. For a UV_{dose} of 1000 mJ cm^{-2}, the % decrease of NO_2^- concentration varies from <10% (Zurich 2, Chicago, Tampa) to >40% (Zurich 1, Lausanne, Perth, Las Vegas, Atlanta) (see Figure S4). Nevertheless, it should be noted that the contribution of NO_2^- to the •OH consumption rate by the wastewater matrix components was usually less than 25%. In most of the studied wastewater effluents, the •OH consumption rate by the matrix components decreases by <10% due to the decrease of NO_2^- for the UV dose of 1000 mJ cm^{-2}. This translates into <11% increase of $[\bullet OH]_{ss}$ compared to the initial condition (i.e., before UV irradiation). Only for the Atlanta wastewater effluent ($[NO_2^-]_0 = 21\ \mu M$), the overall •OH consumption rate by the matrix components decreases by up to 23 % due to the decrease of NO_2^-, indicating up to 30% increase of $[\bullet OH]_{ss}$ compared to the initial condition.

Kinetic modeling of NO_2^- evolution during UV/H_2O_2 treatment. The decrease of NO_2^- during UV/H_2O_2 treatment can be induced by UV photolysis (Eqs. S8 – S10). The molar absorption coefficient of NO_2^- at 254 nm (ε_{NO2-}) is 1 $m^2\ mol^{-1}$.[19] The quantum efficiency of NO_2^- depletion at 254 nm (Φ_{NO2-}) is not clearly known. The quantum efficiency of •OH formation from the NO_2^- photolysis at 280 nm (i.e., Eq. S8) is reported to be 6.8%. However, Eqs. S9 and S10 indicate significant re-formation of NO_2^-. In this study, an estimated value of 3% was used for the Φ_{NO2-}.

$$NO_2^- + h\nu \rightarrow [NO_2^-]^* + H^+ \rightarrow NO\bullet + \bullet OH \quad \text{(S8)}$$

$$NO\bullet + NO_2\bullet \rightarrow N_2O_3 + H_2O \rightarrow 2NO_2^- + 2H^+ \quad \text{(S9)}$$

$$NO\bullet + NO\bullet + O_2 \rightarrow N_2O_4 + H_2O \rightarrow NO_2^- + NO_3^- + 2H^+ \quad \text{(S10)}$$

NO_2^- can be depleted by its reaction with •OH (Eq. S11). The NO_2• from Eq. S11 reacts with another NO_2• via dimerization, which transforms into NO_2^- and NO_3^- (Eq. S12). NO_2• can oxidize electron-rich organic compounds, such as phenolate via a one-electron transfer, thereby forming NO_2^- (Eq. S13). The reaction of NO_2• with O_2•$^-$ is also expected to occur in UV/H_2O_2 process, which re-forms NO_2^- via the short-lived peroxynitrite (Eq. S14). Overall, it is concluded that NO_2^- can scavenge •OH significantly due to its rapid reaction with •OH, but the depletion rate of NO_2^- can be slower than the initial reaction rate of NO_2^- with •OH due to re-formation of NO_2^- from the subsequent reactions of NO_2•.

$$NO_2^- + \bullet OH \rightarrow NO_2\bullet + OH^- \qquad k_{\bullet OH\text{-}NO2^-} = 1\times10^{10}\ M^{-1}\ s^{-1} \qquad (S11)$$

$$NO_2\bullet + NO_2\bullet \rightarrow N_2O_4 + H_2O \rightarrow NO_2^- + NO_3^- + 2H^+ \qquad k_{S11} = 4.5\times10^{8}\ M^{-1}\ s^{-1} \qquad (S12)$$

$$NO_2\bullet + PhO^- \rightarrow NO_2^- + PhO\bullet \qquad k_{S12} = \sim1\times10^{7}\ M^{-1}\ s^{-1} \qquad (S13)$$

$$NO_2\bullet + O_2\bullet^- \rightarrow O_2NOO^- \rightarrow NO_2^- + O_2 \qquad k_{S13} = \sim1\times10^{8}\ M^{-1}\ s^{-1} \qquad (S14)$$

NO_2^- can also be produced from the photolysis of NO_3^- (Eq. S15). The molar absorption coefficient of NO_3^- at 254 nm (ε_{NO3^-}) is 0.3 $m^2\ mol^{-1}$. The quantum efficiency of NO_2^- formation has been known to be 0.03 – 0.1.[19] A value of 0.07 for Φ_{NO3^-} is used in this study as an average value.

$$NO_3^- + hv \rightarrow NO_2^- + 0.5O_2 \qquad (S15)$$

The variation of NO_2^- concentration during UV/H_2O_2 treatment ($[H_2O_2]_0$ = 10 mg/L) was estimated in the 10 municipal wastewater effluents. The •OH consumption rates (i.e., $\sum_i k_{\bullet OH,Si}[S_i]$) were assumed to be constant and equal to the initial consumption rate to simplify the estimation. The fluence-based first-order depletion rate of NO_2^- by UV ($k_{UV\text{-}NO2^-}$) and •OH ($k'_{\bullet OH\text{-}NO2^-}$) can be calculated based on Eqs. S16 and S17. In addition, the fluence-based first-order formation rate of NO_2^- by the photolysis of NO_3^- ($k_{UV\text{-}NO2\text{-}F}$) can be calculated by Eq. S18.

$$k_{UV\text{-}NO2^-} = \frac{2.303\times10}{U}\times\varepsilon_{NO2^-}\times\Phi_{NO2^-} \qquad (S16)$$

$$k'_{\bullet OH\text{-}NO2^-} = \frac{2.303\times10}{U}\times k_{\bullet OH\text{-}NO2^-}\times\frac{\varepsilon_{H2O2}\times\Phi_{\bullet OH,H2O2}\times[H_2O_2]}{\sum_i k_{\bullet OH,Si}[S_i]} \qquad (S17)$$

$$k_{UV\text{-}NO2\text{-}F} = \frac{2.303\times10}{U}\times\varepsilon_{NO3\text{-}}\times\Phi_{NO3\text{-}} \quad \text{(S18)}$$

The UV-dose dependent variation of NO_2^- can be expressed by Eq. S19 in a differential form. The integration of Eq. S19 over UV dose yields Eq. S20 in which $[NO_2^-]_{UVdose}$ is the NO_2^- concentration at a given UV_{dose}, $k_{NO2\text{-}} = k_{UV\text{-}NO2\text{-}} + k'_{\bullet OH\text{-}NO2\text{-}} - k_{UV\text{-}NO2\text{-}F}$, and $N_{tot} = [NO_2^-] + [NO_3^-]$ is the sum of the concentrations of NO_2^- and NO_3^- and is assumed to be constant in time ($N_{tot} = [NO_2^-]_0 + [NO_3^-]_0$).

$$-d[NO_2^-]/dH' = (k_{UV\text{-}NO2\text{-}} + k'_{\bullet OH\text{-}NO2\text{-}})[NO_2^-] + k_{UV\text{-}NO2\text{-}F}[NO_3^-] =$$
$$(k_{UV\text{-}NO2\text{-}} + k'_{\bullet OH\text{-}NO2\text{-}} - k_{UV\text{-}NO2\text{-}F})[NO_2^-] + k_{UV\text{-}NO2\text{-}F}N_{tot} = k_{NO2\text{-}}[NO_2^-] + k_{UV\text{-}NO2\text{-}F}N_{tot} \quad \text{(S19)}$$

$$[NO_2^-]_{H'} = [NO_2^-]_0 \exp(-k_{NO2\text{-}}\times H') + k_{UV\text{-}NO2\text{-}F}N_{tot}/k_{NO2\text{-}}(1-\exp(-k_{NO2\text{-}}\times H')) \quad \text{(S20)}$$

The calculated values of $k_{UV\text{-}NO2\text{-}}$, $k'_{\bullet OH\text{-}NO2\text{-}}$, and $k_{UV\text{-}NO2\text{-}F}$ were used to predict the evolution of NO_2^- as a function of UV_{dose} in each wastewater effluent using Eq. S20, and the results are shown in Figure S4. In all studied cases, the oxidation of NO_2^- by •OH (Eq. S11) was the dominant pathway for the variation of NO_2^-. The photolysis of NO_2^- (Eq. S8) or the formation of NO_2^- by the photolysis of NO_3^- (Eq. S15) were of minor importance. The degree of the NO_2^- decrease was mainly influenced by the initial NO_2^- level and the DOC concentration in which the latter contributes most of the overall •OH scavenging rate. For higher initial NO_2^- levels and lower DOC concentrations, the decrease of NO_2^- became more pronounced. For a UV_{dose} of 1000 mJ/cm^2, where more than an 80% elimination for most micropollutants is achieved, the relative decrease of NO_2^- concentration was ~0 – 65%. However, considering the NO_2^- re-formation pathways from NO_2• (i.e., Eqs. S12 – S14), the actual decrease of NO_2^- concentration is expected to be much smaller. Furthermore, it should be noted that the contribution of NO_2^- to the overall •OH consumption rate by the matrix components was usually below 25%. The calculations show that the overall •OH consumption rate decreases by ~0 – 23% for a UV_{dose} of 1000 mJ/cm^2 compared to the initial conditions. Overall, our calculations show that with most of the wastewater effluents and treatment

conditions, the potential impacts of changes in major water quality parameters were not significant enough to influence the model prediction of micropollutant elimination during UV/H_2O_2 treatment.

SI-Text-6. Impacts of major water matrix components on the micropollutant abatement efficiency by •OH

The water matrix components such as DOC, nitrite (NO_2^-), carbonate species (HCO_3^-/CO_3^{2-}), and bromide (Br^-) can consume •OH and affect the efficiency of micropollutant abatement during UV/H_2O_2 treatment of municipal wastewater effluents. Impacts of these water matrix components on the micropollutant abatement efficiency by •OH can be quantified using Eqs. 2 and 3 in the main text. Here, the sum of •OH consumption rate by these water matrix components (i.e., ($\sum_i k_{\cdot OH,Si}[S_i]$, s^{-1}) determines the steady-state •OH concentration and thus the micropollutant abatement efficiency where $k_{\bullet OH,Si}$ is the second-order rate constant for the reaction of •OH and [S_i] is the concentration of the matrix components. The $k_{\bullet OH,Si}$ taken from literature is: $k_{\bullet OH,DOC} = 2.1\times10^4$ $(mgC/L)^{-1}$ s^{-1},[3] $k_{\bullet OH,HCO_3^-} = 8.5\times10^6$ M^{-1} s^{-1}, $k_{\bullet OH,CO_3^{2-}} = 3.9\times10^8$ M^{-1} s^{-1}, $k_{\bullet OH,NO_2^-} = 1.0\times10^{10}$ M^{-1} s^{-1}, $k_{\bullet OH,Br^-} = 1.1\times10^9$ M^{-1} s^{-1}, and $k_{\bullet OH,NH_3} = 9.0\times10^7$ M^{-1} s^{-1}.[20] The concentration of these components ([S_i]) in municipal wastewater effluents can vary in the following ranges: [DOC] = 3 – 30 mg/L, [NO_2^-] = 0 – 1 mgN/L, [HCO_3^-/CO_3^{2-}] = 0.5 – 5 mM, and [Br^-] = 0 – 1 mg/L. Figure S5 shows the ranges of the calculated •OH consumption rate at pH 7 by each water matrix component considering their concentration ranges in municipal wastewater effluent. It is found that DOC and nitrite are the main •OH consumers while carbonate species and bromide are the minor contributors to the overall •OH consumption rate. Even though municipal wastewater effluent sometimes contain high levels of ammonia (up to 50 mgN/L), the •OH consumption by ammonia species can be neglected due to the very low reactivity of ammonia species toward •OH (Figure S5). Considering $k_{\bullet OH,NH_4^+} = <10^6$ M^{-1} s^{-1} and $k_{\bullet OH,NH_3} = 9.0\times10^7$ M^{-1} s^{-1} (NDRL/NIST Solution Kinetics Database) and $pK_{a,NH_4^+} = 9.25$, the second-order rate constant for the reaction of •OH with ammonia is 5×10^7 M^{-1} s^{-1} and 5×10^6 M^{-1} s^{-1} at pH 7 and 8, respectively.

Using Eqs. 2 and 3, abatement levels of a micropollutant were calculated during UV/H_2O_2 treatment of hypothetical wastewater effluents with varying concentration of DOC (3 – 30 mg/L), NO_2^- (0 – 1 mgN/L), HCO_3^-/CO_3^{2-} (0.5 – 5 mM), and Br^- (0 – 50 mg/L). It was assumed that the

selected hypothetical micropollutant is eliminated only by its reaction with •OH with a second-order rate constant of 10^{10} M^{-1} s^{-1}. Figure S6 shows that the % abatement levels of the selected micropollutant decrease significantly with increasing concentration of DOC and nitrite while changes little in the cases of carbonate species, and bromide (up to 1 mg/L). For bromide, however, the abatement levels decrease significantly when the bromide concentration increases to 50 mg/L (Fig. 6d). Such extremely high concentration of bromide in municipal wastewater effluent was reported in a recent study.[21]

SI-Text-7. Energy requirement for micropollutant abatement by ozonation

The energy required for the abatement of micropollutants during treatment of a representative wastewater effluent ([DOC] = 6 mgC L^{-1}) with ozone was calculated based on the following procedure. Based on a previous study,[3] the specific O_3 doses required for % micropollutant abatement could be obtained and are summarized in Table S4. The average energy requirement of 0.015 kWh/g of O_3 was used in this study.[22] Therefore, the energy required to treat a cubic meter of water (kWh/m^3) for a given specific ozone dose can be calculated as E_{O3} (kWh m^{-3}) = $0.015\times(O_3/DOC)\times([DOC])$.

SI-Text-8. Energy requirement for micropollutant abatement by the O_3/H_2O_2-UV/H_2O_2 process

A combined process of O_3/H_2O_2 followed by UV/H_2O_2 can be used to minimize bromate formation and achieve sufficient abatement of micropollutants (e.g., NDMA) with reasonable energy consumption. In this process combination, a majority of the micropollutant abatement is achieved in the presence of O_3 with excess H_2O_2 (e.g., mol-H_2O_2/mol-O_3 > 2) to minimize bromate formation.

The residual H_2O_2 from the O_3/H_2O_2 can be used for the post UV/H_2O_2 to achieve additional micropollutant abatement. The molar consumption of H_2O_2 compared to O_3 during O_3/H_2O_2 treatment of wastewater effluent was reported to be ~0.2 (i.e., $\Delta[H_2O_2]/\Delta[O_3]$ = ~0.2, Lee et al., 2013). NDMA, if originally present or formed during ozonation, and other residual micropollutants present after ozonation can be attenuated in the post UV/H_2O_2 process. Due to the water absorbance decrease by ozonation (e.g., 30 – 60% decrease for gO3/gDOC of 0.5 – 1.5),[8] the required energy to deliver the given UV fluence can decrease.[23]

Based on the above descriptions, the energy consumption for the process options of UV/H_2O_2, O_3/H_2O_2, O_3 + UV and O_3/H_2O_2 + UV/H_2O_2 was calculated. The O_3 dose of 3 mg L^{-1} (gO_3/gDOC = 0.5) was selected to achieve significant abatement of ozone-reactive micropollutants while limiting high bromate formation. The H_2O_2 dose for UV/H_2O_2 or O_3/H_2O_2 was 5 mg L^{-1}. The O_3/H_2O_2 option was considered instead of the O_3 without H_2O_2 to further lower the bromate formation. It was assumed that 20% of the H_2O_2 applied for O_3/H_2O_2 is consumed and the remaining 80% of the applied H_2O_2 can be used for the downstream UV/H_2O_2 process. Finally, the UV dose of 360 mJ cm^{-2} was applied to achieve 80% NDMA abatement. It was assumed that the pre-ozonation for the gO_3/gDOC of 0.5 increases the UV transmittance of the water at 254 nm by 30 %.

The details of the calculations are:

1) UV/H_2O_2: $E = E_{lamp} + E_{H2O2} = 0.108 + 0.05 = 0.158$ kWh m^{-3}

$E_{lamp} = \frac{H^0/WF}{L\times\eta_{UV}\times(3600)} = \frac{H^0}{L\times\eta_{UV}\times(3600)}\times\frac{(1-10^{-A254nm\times L})}{2.303\times A_{254nm}\times L} = 0.108$ kWh m^{-3} in which $H' = 360$ mJ cm^{-2}, L = 10 cm, $\eta_{UV} = 0.3$, and $A_{254nm} = 0.132$ cm^{-1}.

$E_{H2O2} = \eta_{H2O2}\times[H_2O_2]_0 = 0.05$ kWh m^{-3} in which $\eta_{H2O2} = 0.01$ kWh g^{-1} and $[H_2O_2]_0 = 5$ g m^{-3}

2) O_3/H_2O_2: $E = E_{O3} + E_{H2O2} = 0.045 + 0.05 = 0.095$ kWh m^{-3}

$E_{O3} = \eta_{O3}\times[O_3]_0 = 0.045$ kWh m^{-3} in which $\eta_{O3} = 0.015$ kWh g^{-1} and $[O_3]_0 = 3$ g m^{-3}

$E_{H2O2} = \eta_{H2O2}\times[H_2O_2]_0 = 0.05$ kWh m^{-3} in which $\eta_{H2O2} = 0.01$ kWh g^{-1} and $[H_2O_2]_0 = 5$ g m^{-3}

3) O_3 + UV: $E = E_{O3} + E_{lamp} = 0.045 + 0.0805 = 0.126$ kWh m^{-3}

$E_{O3} = \eta_{O3}\times[O_3]_0 = 0.045$ kWh m^{-3} in which $\eta_{O3} = 0.015$ kWh g^{-1} and $[O_3]_0 = 3$ g m^{-3}

$E_{lamp} = \frac{H^0/WF}{L\times\eta_{UV}\times(3600)} = \frac{H^0}{L\times\eta_{UV}\times(3600)}\times\frac{(1-10^{-A254nm\times L})}{2.303\times A_{254nm}\times L} = 0.0805$ kWh m^{-3} in which $H' = 360$ mJ cm^{-2}, L = 10 cm, $\eta_{UV} = 0.3$, and $A_{254nm} = 0.0924$ cm^{-1} (30% decrease from 0.132 by pre-ozonation) cm^{-1}.

4) O_3/H_2O_2 + UV/H_2O_2: $E = E_{O3} + E_{H2O2} + E_{lamp} = 0.045 + 0.05 + 0.0805 = 0.176$ kWh m^{-3}

$E_{O3} = \eta_{O3}\times[O_3]_0 = 0.045$ kWh m^{-3} in which $\eta_{O3} = 0.015$ kWh g^{-1} and $[O_3]_0 = 3$ g m^{-3}

$E_{H2O2} = \eta_{H2O2}\times[H_2O_2]_0 = 0.05$ kWh m^{-3} in which $\eta_{H2O2} = 0.01$ kWh g^{-1} and $[H_2O_2]_0 = 5$ g m^{-3}

$E_{lamp} = \frac{H^0/WF}{L \times \eta_{UV} \times (3600)} = \frac{H^0}{L \times \eta_{UV} \times (3600)} \times \frac{(1 - 10^{-A254nm \times L})}{2.303 \times A_{254nm} \times L}$ = 0.0805 kWh m^{-3} in which H′ = 360 mJ cm^{-2}, L = 10 cm, $\eta_{UV} = 0.3$, and A_{254nm} = 0.0924 cm^{-1} (30% decrease from 0.132 by pre-ozonation) cm^{-1}.

Table S1. Summary of water quality parameters of wastewater effluents and the •OH reaction rate constant with EfOM

Effluent sample location	pH	DOC, mg-C L^{-1}	Alkalinity, mg L^{-1} as $CaCO_3$	NO_2^-, mg-N L^{-1}	NO_3^-, mg-N L^{-1}	Br^-, μg L^{-1}	A_{254nm}, cm^{-1}	ε_{DOC} or $SUVA_{254nm}$, $(mgC/L)^{-1}$ cm^{-1}[a]	$k_{•OH/EfOM}$, $(mgC/L)^{-1}$ s^{-1}[b]	$\sum_i k_{Si}[S_i]$, s^{-1}[c]
	Switzerland (CH)									
Zurich 1	7.0	4.7	145	0.07	13.2	37	0.11	0.023	2.0×10^4	1.7×10^5
Zurich 2	7.2	4.7	220	0.01	12.0	40	0.13	0.028	2.0×10^4	1.4×10^5
Lausanne	7.2	6.0	65	0.16	24.0	940	0.10	0.017	1.9×10^4	2.6×10^5
	Australia (AUS)									
Brisbane	7.3	26.4	295	0.45	0.20	140	0.41	0.016	1.0×10^4	6.4×10^5
Perth	7.1	7.0	105	0.05	18.0	330	0.20	0.029	2.0×10^4	2.0×10^5
	United States (U.S.)									
Las Vegas	6.9	7.1	123	0.06	14.0	174	0.15	0.021	1.8×10^4	2.0×10^5
Chicago	7.6	5.7	134	<0.05	9.10	93	0.13	0.023	2.7×10^4	1.8×10^5
Los Angeles	7.3	15.0	332	0.17	0.11	409	0.28	0.019	2.2×10^4	5.2×10^5
Tampa	7.3	7.0	205	<0.05	7.70	730	0.19	0.027	2.3×10^4	2.1×10^5
Atlanta	7.3	6.3	169	0.30	8.60	31	0.13	0.021	3.4×10^4	4.6×10^5

[a]the average value of ε_{DOC} (i.e., $SUVA_{254nm} = A_{254nm}/[DOC]$) for the tested 10 wastewater effluents was 0.022±0.004, [b]from Lee et al., 2013,[3] [c]•OH scavenging rate (s^{-1}) calculated as $\sum_i k_{Si}[S_i] = k_{•OH/EfOM}[DOC] + k_{•OH/HCO3-}[HCO_3^-] + k_{•OH/CO32-}[CO_3^{2-}] + k_{•OH/NO2-}[NO_2^-] + k_{•OH/Br-}[Br^-]$.

Table S2. Summary of the photolysis rate constants during treatment with UV alone ($k_{UV\text{-}meas}$; mJ^{-1} cm^2) and UV/H_2O_2 ($k_{UV/H2O2\text{-}meas}$; mJ^{-1} cm^2) and the % contribution of UV to the overall micropollutant abatement. An initial H_2O_2 concentration of 10 mg L^{-1} was applied for the UV/H_2O_2.

Compound		Zurich 1	Zurich 2	Lausanne	Brisbane	Perth	Las Vegas	Chicago	Los Angeles	Tampa	Atlanta	Average
Diclofenac	$k_{UV\text{-}meas}$	4.67E-3	5.40E-3	4.69E-3	2.06E-3	5.01E-3	1.17E-2	8.99-3	1.02E-2	1.00E-2	9.62E-3	(7.2±3.2) E-3
	$k_{UV/H2O2\text{-}meas}$	7.30E-3	5.08E-3	5.28E-3	1.84E-3	5.41E-3	1.33E-2	1.13E-2	9.56E-3	9.21E-3	9.21E-3	–
	%	64	~100	89	~100	93	88	80	~100	~100	~100	91±12
NDMA	$k_{UV\text{-}meas}$	N.A.	N.A.	N.A.	N.A.	N.A.	5.18E-3	4.61E-3	4.90E-3	4.03E-3	3.95E-3	(4.5±0.5) E-3
	$k_{UV/H2O2\text{-}meas}$	N.A.	N.A.	N.A.	N.A.	N.A.	4.05E-3	4.38E-3	5.46E-3	4.08E-3	3.52E-3	–
	%	N.A.	N.A.	N.A.	N.A.	N.A.	~100	~100	90	~100	~100	~100
Triclosan	$k_{UV\text{-}meas}$	2.22E-3	2.66E-3	3.03E-3	1.53E-3	2.23E-3	9.25E-3	5.33E-3	4.83E-3	8.91E-3	5.81E-3	(4.6±2.8) E-3
	$k_{UV/H2O2\text{-}meas}$	3.92E-3	2.77E-3	3.92E-3	1.39E-3	2.08E-3	1.00E-2	6.34E-3	4.93E-3	7.57E-3	5.60E-3	–
	%	57	96	77	~100	~100	93	84	98	~100	89	90±14
Sulfamethoxazole	$k_{UV\text{-}meas}$	1.75E-3	1.76E-3	1.38E-3	1.27E-3	1.48E-3	2.85E-3	2.54E-3	2.32E-3	2.02E-3	2.29E-3	(2.0±0.5) E-3
	$k_{UV/H2O2\text{-}meas}$	2.66E-3	2.02E-3	1.53E-3	1.01E-3	1.72E-3	3.78E-3	3.06E-3	2.34E-3	2.18E-3	2.28E-3	–
	%	66	87	90	~100	86	75	83	99	93	100	88±11
Phenytoin	$k_{UV\text{-}meas}$	7.77E-4	9.65E-4	8.28E-4	8.12E-4	8.57E-4	1.88E-3	1.27E-3	1.64E-3	1.24E-3	9.13E-4	(1.1±0.4) E-3
	$k_{UV/H2O2\text{-}meas}$	2.04E-3	1.82E-3	1.43E-3	7.81E-4	1.68E-3	3.61E-3	1.75E-3	1.67E-3	1.78E-3	1.37E-3	–
	%	38	53	58	~100	51	52	73	98	70	67	66±20
Atrazine	$k_{UV\text{-}meas}$	4.77E-4	6.56E-4	6.53E-4	4.85E-4	6.10E-4	1.16E-3	6.23E-4	5.83E-4	9.56E-4	9.10E-4	(7.1±2.2) E-4
	$k_{UV/H2O2\text{-}meas}$	9.14E-4	8.87E-4	8.43E-4	6.02E-4	1.01E-3	1.29E-3	5.60E-4	6.74E-4	1.01E-3	9.24E-4	–
	%	52	74	77	81	60	90	~100	86	95	98	83±18
Naproxen	$k_{UV\text{-}meas}$	2.81E-4	3.78E-4	3.01E-4	2.98E-4	2.81E-4	6.29E-4	0	3.15E-4	3.25E-4	5.63E-4	(3.4±1.7) E-4
	$k_{UV/H2O2\text{-}meas}$	1.68E-3	1.61E-3	1.16E-3	4.98E-4	1.24E-3	2.27E-3	6.66E-4	6.62E-4	1.08E-3	9.84E-4	–
	%	17	23	26	60	23	28	0	48	30	57	31±19
Ibuprofen	$k_{UV\text{-}meas}$	1.09E-4	1.76E-4	1.35E-4	7.09E-5	1.45E-4	N.A.	N.A.	N.A.	N.A.	N.A.	(1.3±0.4) E-4

	$k_{UV/H2O2-meas}$	1.17E-3	1.20E-3	8.33E-4	2.56E-4	8.92E-4	1.44E-3	2.72E-4	6.24E-4	8.00E-4	5.86E-4	–
	%	9	15	16	28	16	N.A.	N.A.	N.A.	N.A.	N.A.	17±7
Bisphenol A	$k_{UV-meas}$	4.54E-5	1.79E-4	3.41E-4	6.40E-5	1.60E-4	N.A.	N.A.	N.A.	N.A.	N.A.	(1.6±1.2) E-4
	$k_{UV/H2O2-meas}$	1.43E-3	1.30E-3	1.31E-3	2.66E-4	9.80E-4	2.70E-3	5.33E-4	2.86E-4	1.19E-3	3.64E-4	–
	%	3	14	26	24	16	N.A.	N.A.	N.A.	N.A.	N.A.	17±9
Carbamazepine	$k_{UV-meas}$	4.81E-5	8.06E-5	1.28E-4	0	9.33E-5	N.A.	N.A.	N.A.	N.A.	N.A.	(7.0±4.8) E-5
	$k_{UV/H2O2-meas}$	1.23-3	1.26E-3	9.30E-4	1.93E-4	1.01E-3	1.58E-3	6.11E-4	N.A	1.24E-3	2.81E-4	–
	%	4	6	14	0	9	N.A.	N.A.	N.A.	N.A.	N.A.	7±5
Primidone	$k_{UV-meas}$	N.A.	7.75E-5	8.00E-5	N.A.	7.57E-5	N.A.	N.A.	N.A.	N.A.	N.A.	(7.8±0.2) E-5
	$k_{UV/H2O2-meas}$	8.36E-4	1.05E-3	6.33E-4	1.37E-4	5.98E-4	6.42E-4	2.72E-4	N.A.	6.70E-4	2.10E-4	–
	%	N.A.	7	13	N.A.	13	N.A.	N.A.	N.A.	N.A.	N.A.	11±3
Atenolol	$k_{UV-meas}$	7.14E-5	N.A.	N.A.	8.69E-5	N.A.	N.A.	N.A.	N.A.	N.A.	N.A.	(7.1±2.2) E-5
	$k_{UV/H2O2-meas}$	1.01E-3	1.17E-3	7.38E-4	1.40E-4	8.10E-3	1.34E-3	N.A.	N.A.	6.81E-4	5.85E-4	–
	%	5	N.A.	N.A.	11	N.A.	N.A.	N.A.	N.A.	N.A.	N.A.	8±4
Trimethoprim	$k_{UV-meas}$	6.40E-5	1.38E-4	2.76E-5	N.A.	8.07E-5	N.A.	N.A.	N.A.	N.A.	N.A.	(7.8±4.6) E-5
	$k_{UV/H2O2-meas}$	1.15E-3	1.18E-3	7.39E-4	1.75E-4	8.99E-4	1.18E-3	3.84E-4	2.53E-4	4.60E-4	4.39E-4	–
	%	6	12	4	N.A.	9	N.A.	N.A.	N.A.	N.A.	N.A.	7±4
Gemfibrozil	$k_{UV-meas}$	2.95E-5	7.50E-5	8.02E-5	2.85E-5	8.73E-5	N.A.	N.A.	N.A.	N.A.	N.A.	(6.0±2.9) E-5
	$k_{UV/H2O2-meas}$	1.11E-3	1.13E-3	8.31E-4	2.08E-4	9.61E-4	1.62E-3	3.71E-4	4.96E-4	6.65E-4	5.85E-4	–
	%	3	7	10	14	9	N.A.	N.A.	N.A.	N.A.	N.A.	8±4
DEET	$k_{UV-meas}$	7.66E-5	6.95E-5	2.75E-5	N.A.	N.A.	N.A.	N.A.	N.A.	N.A.	N.A.	(5.8±2.7) E-5
	$k_{UV/H2O2-meas}$	9.94E-4	9.71E-4	5.58E-4	1.22E-4	5.74E-4	1.01E-3	2.82E4	5.61E-4	4.39E-4	4.96E-4	–
	%	8	7	5	N.A.	N.A.	N.A.	N.A.	N.A.	N.A.	N.A.	7±1
Meprobamate	$k_{UV-meas}$	N.A.	N.A.	N.A.	N.A.	N.A.	N.A.	N.A.	N.A.	N.A.	N.A.	0
	$k_{UV/H2O2-meas}$	5.32E-4	5.41E-4	3.99E-4	1.12E-4	3.59E-4	5.43E-4	N.A.	9.14E-4	3.33E-4	3.80E-4	–
	%	0	0	0	0	0	0	0	0	0	0	0

Table S3. Summary of the molar absorptivity (ε_{MP}) and quantum yield (Φ_{MP}) at 254nm, and second-order rate constant with •OH ($k_{\bullet OH,MP}$) for the selected micropollutants.

compound	ε_{MP}, m^2 mol^{-1}	Φ_{MP} mol $einstein^{-1}$	$k_{\bullet OH,MP}$, M^{-1} s^{-1} g	Ref.
Diclofenac	5.2×10^2	0.21 (pH 7.8)	9.3×10^9	Baeza and Knappe, 2011[24]
	6.1×10^2	0.28 (pH 7)		Meite et al., 2010[25]
	4.3×10^2	0.38 (pH 7)		Canonica et al., 2008[11]
			7.5×10^9	Huber et al., 2003[26]
	5.2×10^2	**0.29**	**8.4×10^9**	Values used in this study
NDMA	1.65×10^2	0.31 (pH 3-8)		Lee et al., 2005[27]
	1.40×10^2	0.30 (pH 8)		Sharpless and Linden, 2003[28]
		0.13 (pH 7) (excluded as an outlier)		Ho et al., 1996[29]
			4.5×10^8	Lee et al., 2007[30]
			3.3×10^8	Wink et al., 1991[31]
			4.3×10^8	Mezyk et al., 2004[32]
	1.53×10^2	**0.31**	**4.0×10^8**	Values used in this study
Triclosan		0.28 (pH 6.4)		Wong-Wah-Chung et al., 2007[33]
	1.95×10^2			Measured in this study
			9.6×10^9	Lee and von Gunten, 2012[34]
			5.4×10^9	Latch et al., 2005[35]
	1.95×10^2	**0.28**	**7.5×10^9**	Values used in this study
Sulfamethoxazole	1.66×10^3	2.97×10^{-2} (pH 7.8)	5.6×10^9	Baeza and Knappe, 2011[24]
	1.68×10^3	4.6×10^{-2} (pH 7.8)		Canonica et al., 2008[11]

	1.19×10^{3}			Azrague and Osterhus, 2009[36]
			5.5×10^{9}	Huber et al., 2003[26]
			8.5×10^{9}	Mezyk et al., 2007[37]
	1.51×10^{3}	**3.79×10^{-2}**	**6.5×10^{9}**	Values used in this study
Phenytoin	1.26×10^{2}	2.79×10^{-1} (pH 7.0)	6.3×10^{9}	Yuan et al., 2009[38]
	1.26×10^{2}	**2.79×10^{-1}**	**6.3×10^{9}**	Values used in this study
Atrazine	3.68×10^{2}	3.3×10^{-2}		Bolton and Stefan, 2002[13]
	3.86×10^{2}	5.0×10^{-2}		Nick et al., 1992[39]
	2.65×10^{2}	6.0×10^{-2}		Sanches et al., 2010[40]
	3.86×10^{2}	4.6×10^{-2} (pH 7)		Canonica et al., 2008[11]
			2.4×10^{9}	De Laat et al., 1994[41]
			3.0×10^{9}	Acero et al., 2000[42]
	3.51×10^{2}	**4.73×10^{-2}**	**2.7×10^{9}**	Values used in this study
Naproxen	3.2×10^{2}	5.0×10^{-2}	8.4×10^{9}	Benitez et al., 2009[43]
	3.95×10^{2}	2.4×10^{-2}		Meite et al., 2010[25]
	4.9×10^{2}	9.3×10^{-3}	8.6×10^{9}	Pereira et al., 2007[44]
	4.2×10^{2}	1.3×10^{-2}		Marotta et al., 2013[45]
			9.6×10^{9}	Packer et al., 2003[46]
	4.06×10^{2}	**2.78×10^{-2}**	**8.9×10^{9}**	Values used in this study
Ibuprofen	25.6	1.92×10^{-1}	6.7×10^{9}	Yuan et al., 2009[38]
			7.4×10^{9}	Huber et al., 2003[26]
	25.6	**1.92×10^{-1}**	**7.1×10^{9}**	Values used in this study
Bisphenol-A	75	4.6×10^{-3}	5.8×10^{9}	Baeza and Knappe, 2011[24]
		8.5×10^{-3}	1.0×10^{10}	Resenfeldt and Linden,

				2004[47]
	75	**4.6×10^{-3}**	**7.9×10^{9}**	Values used in this study
Carbamazepine	6.07×10^{2}	6.0×10^{-4}	5.9×10^{9}	Pereira et al., 2007[44]
			8.8×10^{9}	Huber et al., 2003[26]
			9.4×10^{9}	Lam and Mabury, 2005[48]
	6.07×10^{2}	**6.0×10^{-4}**	**8.9×10^{9}**	Values used in this study
Primidone	22	8.2×10^{-2}	6.7×10^{9}	Real et al., 2009[49]
	22	**8.2×10^{-2}**	**6.7×10^{9}**	Values used in this study
Atenolol	43			Measured in this study
			8.0×10^{9}	Benner et al., 2008[50]
	43		**8.0×10^{9}**	Values used in this study
Trimethoprim	2.94×10^{2}	1.18×10^{-3}	5.7×10^{9}	Baeza and Knappe, 2011[24]
			6.9×10^{9}	Dodd et al., 2006[51]
	2.94×10^{2}	**1.18×10^{-3}**	**6.3×10^{9}**	Values used in this study
Gemfibrozil	27			Measured in this study
			10×10^{9}	Razavi et al., 2009[52]
	27		**10×10^{9}**	Values used in this study
DEET	1.29×10^{2}			Measured in this study
			5.0×10^{9}	Song et al., 2009[53]
	1.29×10^{2}		**5.0×10^{9}**	Values used in this study
Meprobamate			3.7×10^{9}	Lee et al., 2013[3]
			3.7×10^{9}	Values used in this study

Table S4. Specific ozone doses (O_3/DOC) and the corresponding energy (E_{O3}, kWh m^{-3}) required for the specific percent micropollutant abatement during ozonation of a municipal wastewater effluent. The wastewater effluent contains 6 mgC L^{-1} of DOC and pH 7. The calculations were based on the data provided in Lee et al., 2013.[3]

micropollutant group based on the ozone reactivity	20% elimination	40% elimination	60% elimination	80% elimination	90% elimination
Group I (triclosan, diclofenac, bisphenol A, sulfamethoxazole, carbamazepine, trimethoprim, naproxen)	O_3/DOC = 0.06, E_{O3} = 0.005 kWh m^{-3}	O_3/DOC = 0.12, E_{O3} = 0.011 kWh m^{-3}	O_3/DOC = 0.18, E_{O3} = 0.016 kWh m^{-3}	O_3/DOC = 0.24, E_{O3} = 0.022 kWh m^{-3}	O_3/DOC = 0.27, E_{O3} = 0.024 kWh m^{-3}
Group II (gemfibrozil)	O_3/DOC = 0.07, E_{O3} = 0.006 kWh m^{-3}	O_3/DOC = 0.14, E_{O3} = 0.013 kWh m^{-3}	O_3/DOC = 0.21, E_{O3} = 0.019 kWh m^{-3}	O_3/DOC = 0.28, E_{O3} = 0.025 kWh m^{-3}	O_3/DOC = 0.32, E_{O3} = 0.029 kWh m^{-3}
Group II (atenolol)	O_3/DOC = 0.1, E_{O3} = 0.009 kWh m^{-3}	O_3/DOC = 0.2, E_{O3} = 0.018 kWh m^{-3}	O_3/DOC = 0.3, E_{O3} = 0.027 kWh m^{-3}	O_3/DOC = 0.4, E_{O3} = 0.036 kWh m^{-3}	O_3/DOC = 0.45, E_{O3} = 0.041 kWh m^{-3}
Group III (ibuprofen, phenytoin, DEET, primidone)	O_3/DOC = 0.2, E_{O3} = 0.018 kWh m^{-3}	O_3/DOC = 0.4, E_{O3} = 0.036 kWh m^{-3}	O_3/DOC = 0.6, E_{O3} = 0.054 kWh m^{-3}	O_3/DOC = 0.8, E_{O3} = 0.072 kWh m^{-3}	O_3/DOC = 1.0, E_{O3} = 0.090 kWh m^{-3}
Group IV (meprobamate, atrazine)	O_3/DOC = 0.25, E_{O3} = 0.023 kWh m^{-3}	O_3/DOC = 0.5, E_{O3} = 0.045 kWh m^{-3}	O_3/DOC = 0.8, E_{O3} = 0.072 kWh m^{-3}	O_3/DOC = 1.4, E_{O3} = 0.126 kWh m^{-3}	O_3/DOC = 1.7, E_{O3} = 0.153 kWh m^{-3}

Figure S1. Measured and predicted percent abatement of the selected micropollutants as a function of UV dose during treatment of the wastewater effluents with UV (triangles and dashed lines) and UV/H_2O_2 (circles and solid lines) ($[H_2O_2]_0$ = 10 mg L^{-1}). Symbols and lines represent the measured and predicted data, respectively.

(a) diclofenac

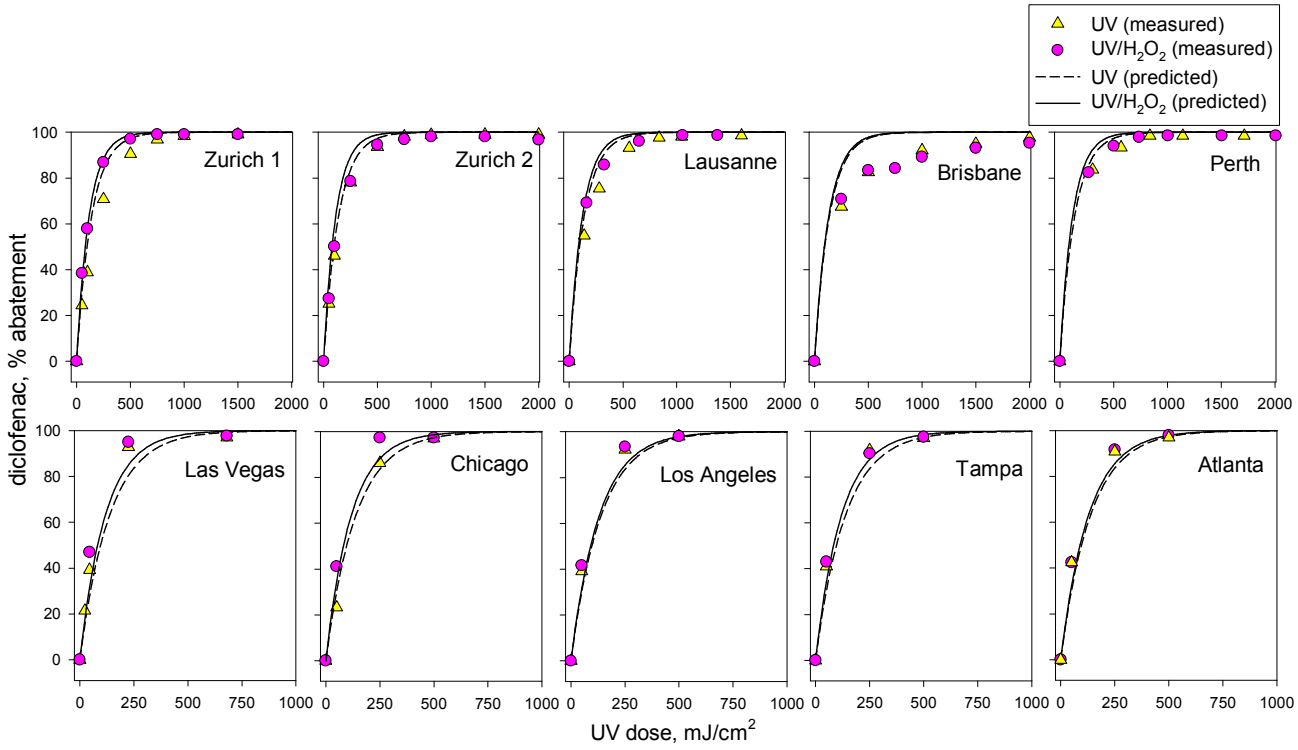

(b) NDMA

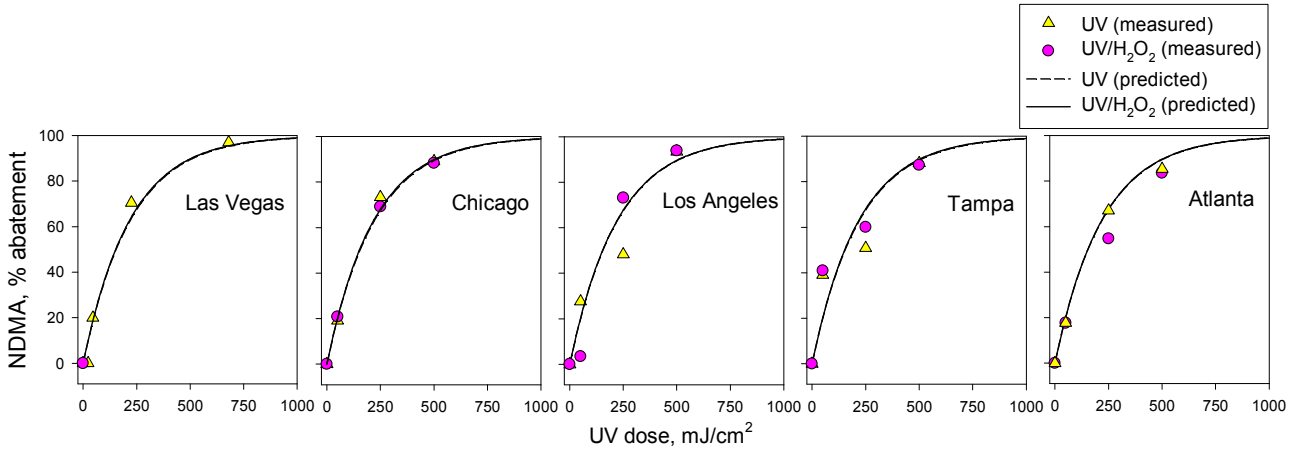

(c) triclosan

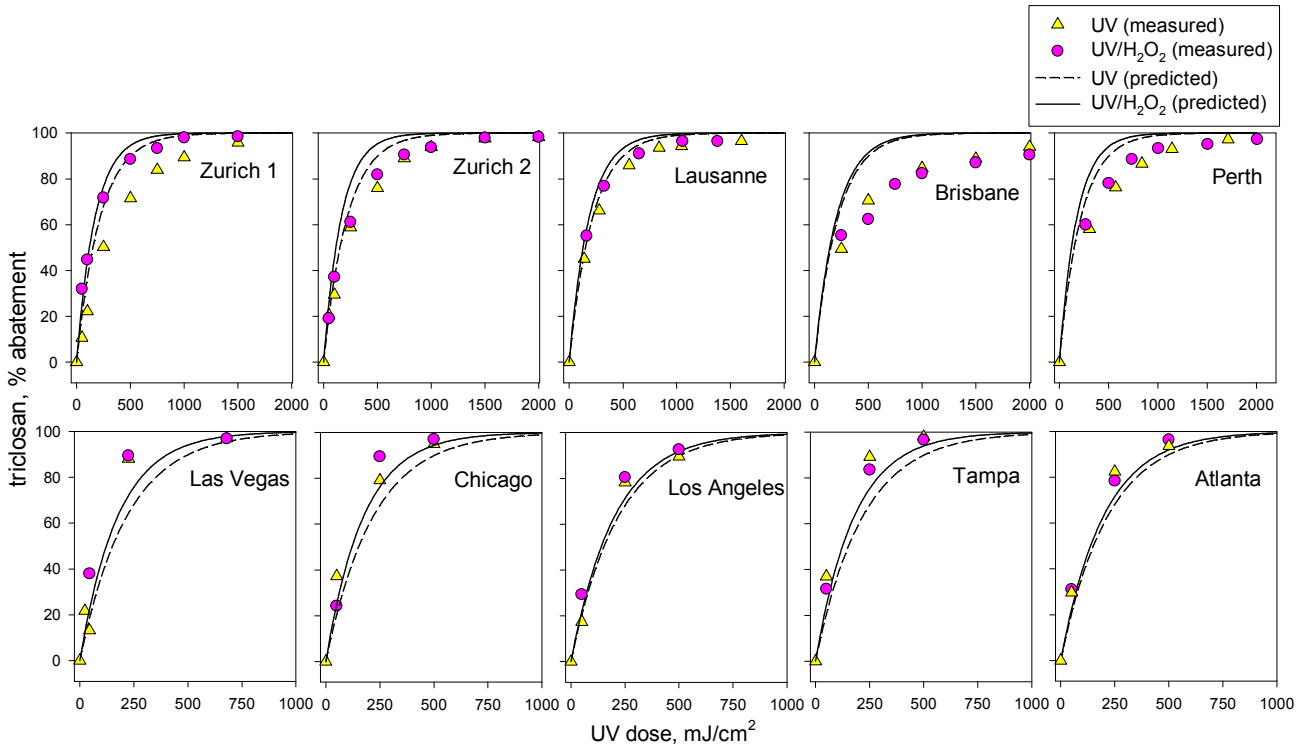

(d) sulfamethoxazole

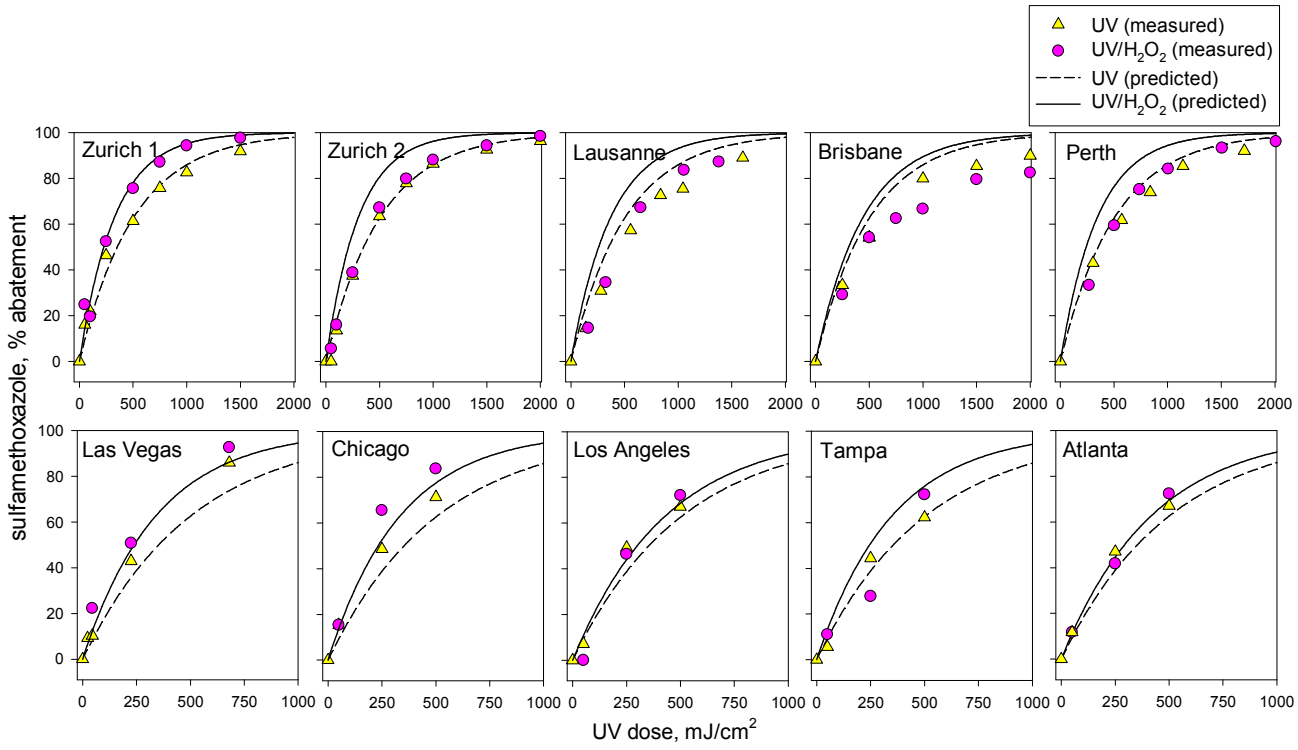

(e) phenytoin

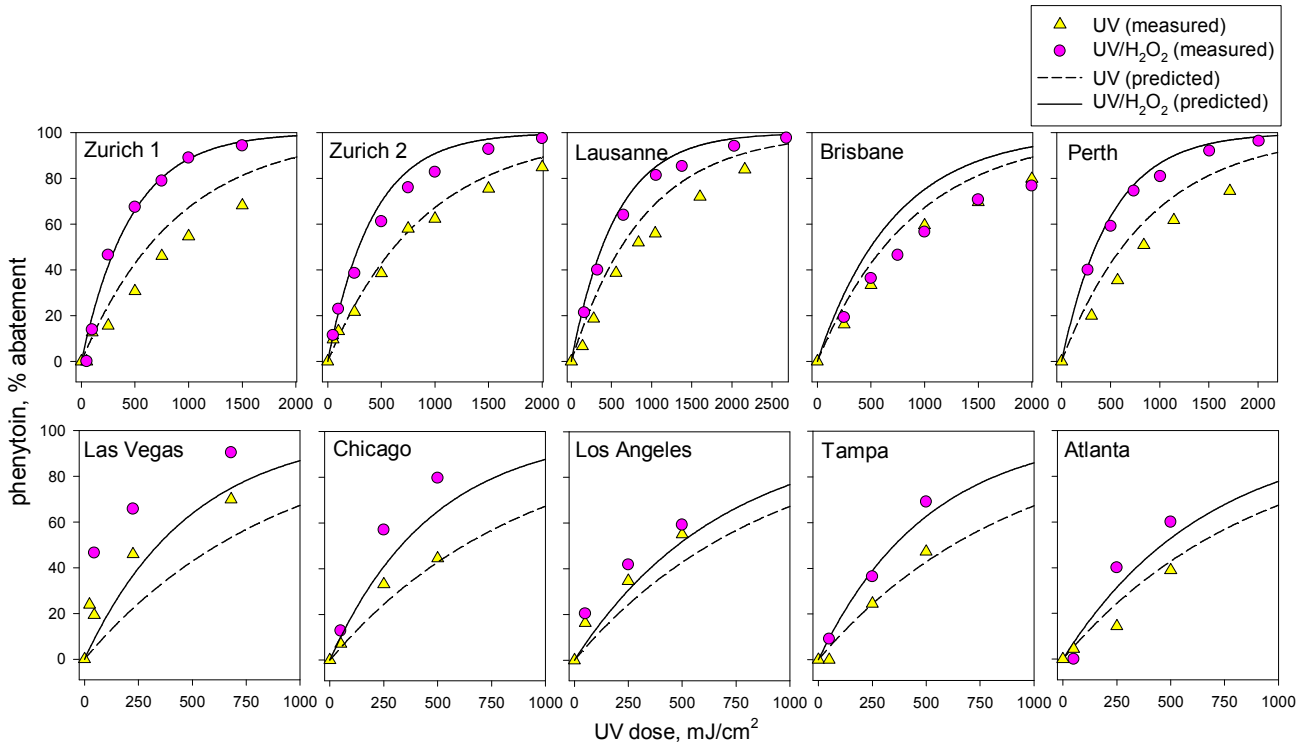

(f) atrazine

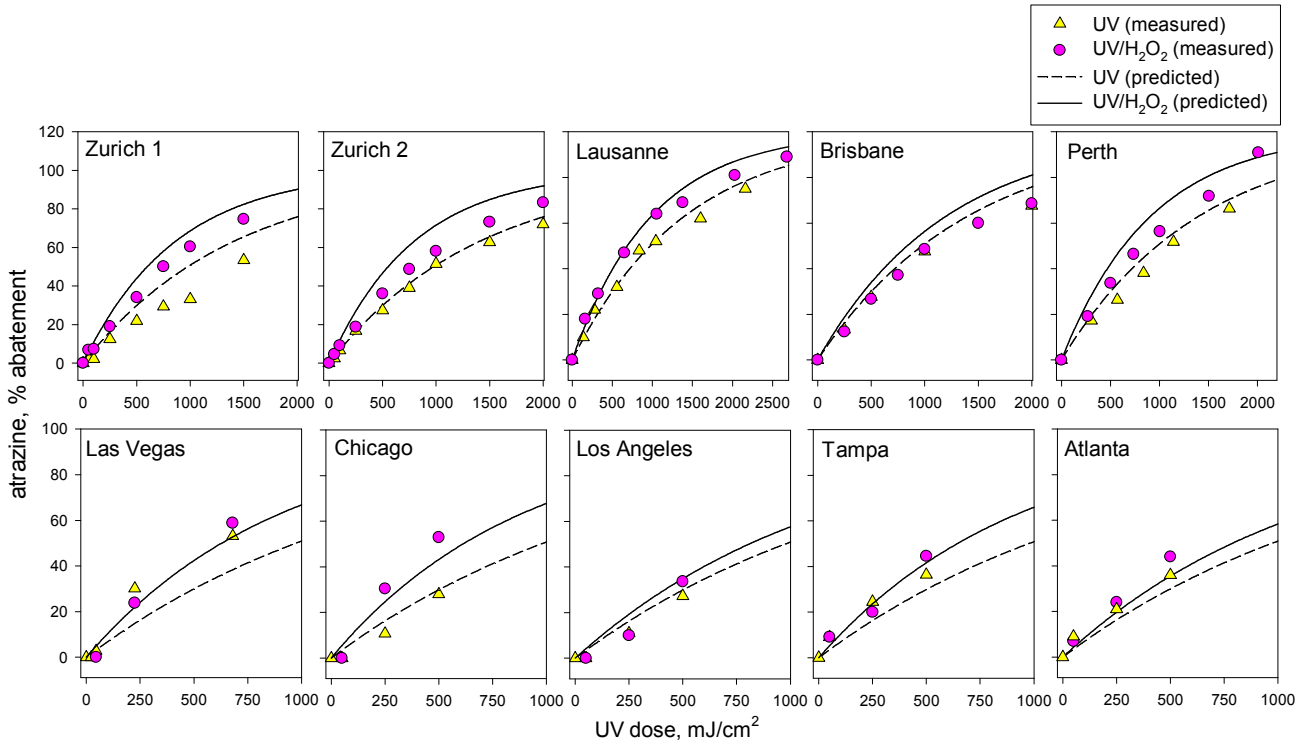

(g) naproxen

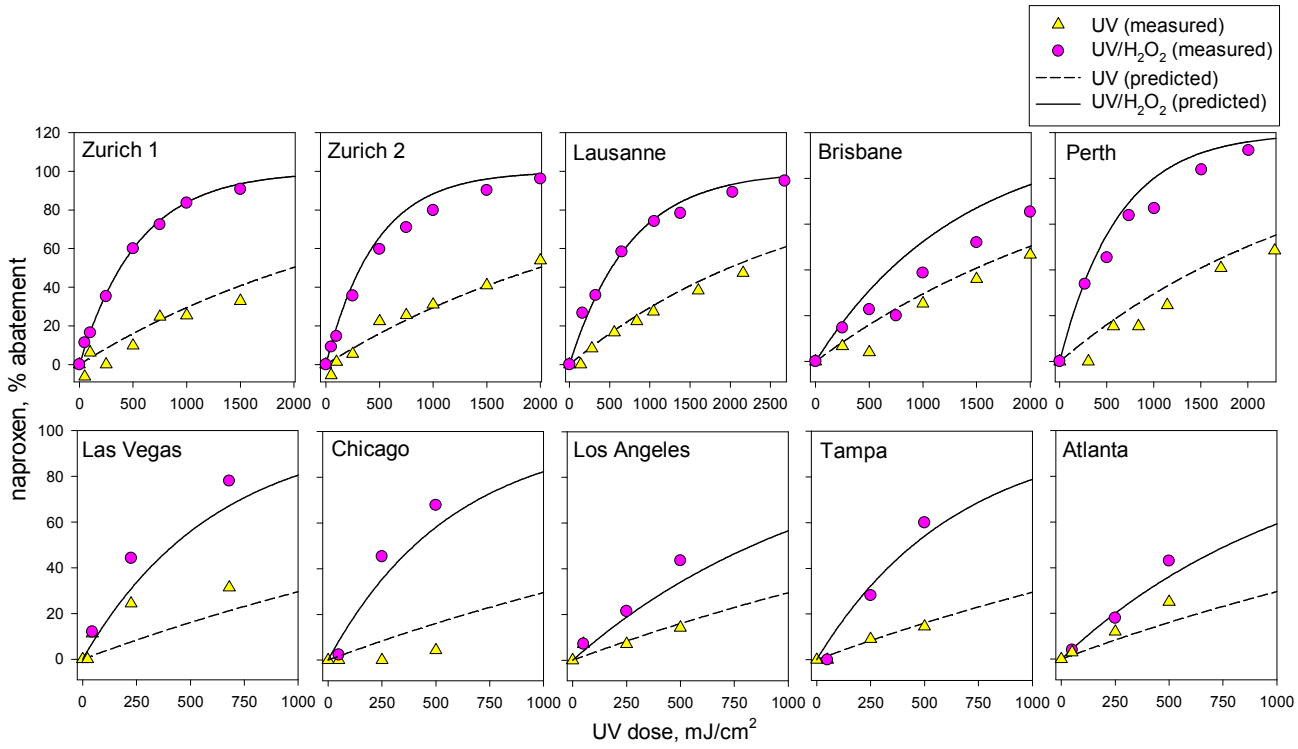

(h) ibuprofen

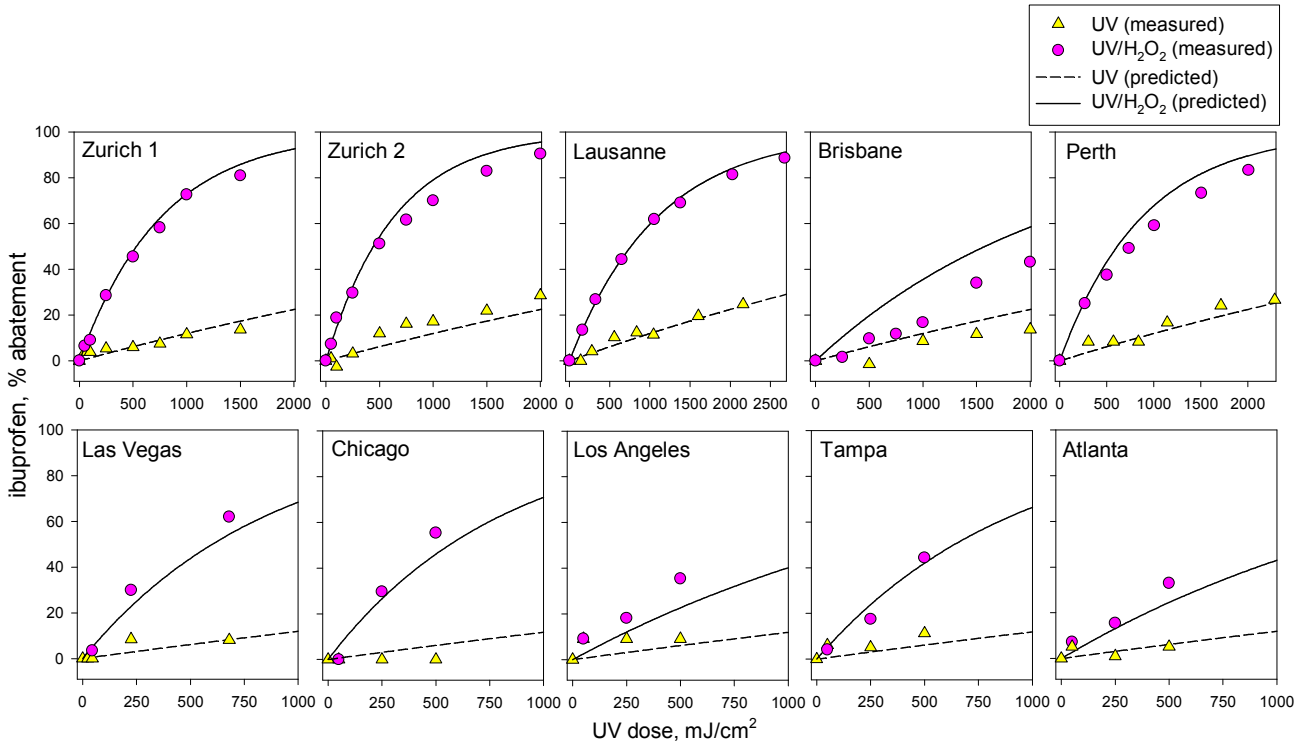

(i) bisphenol A

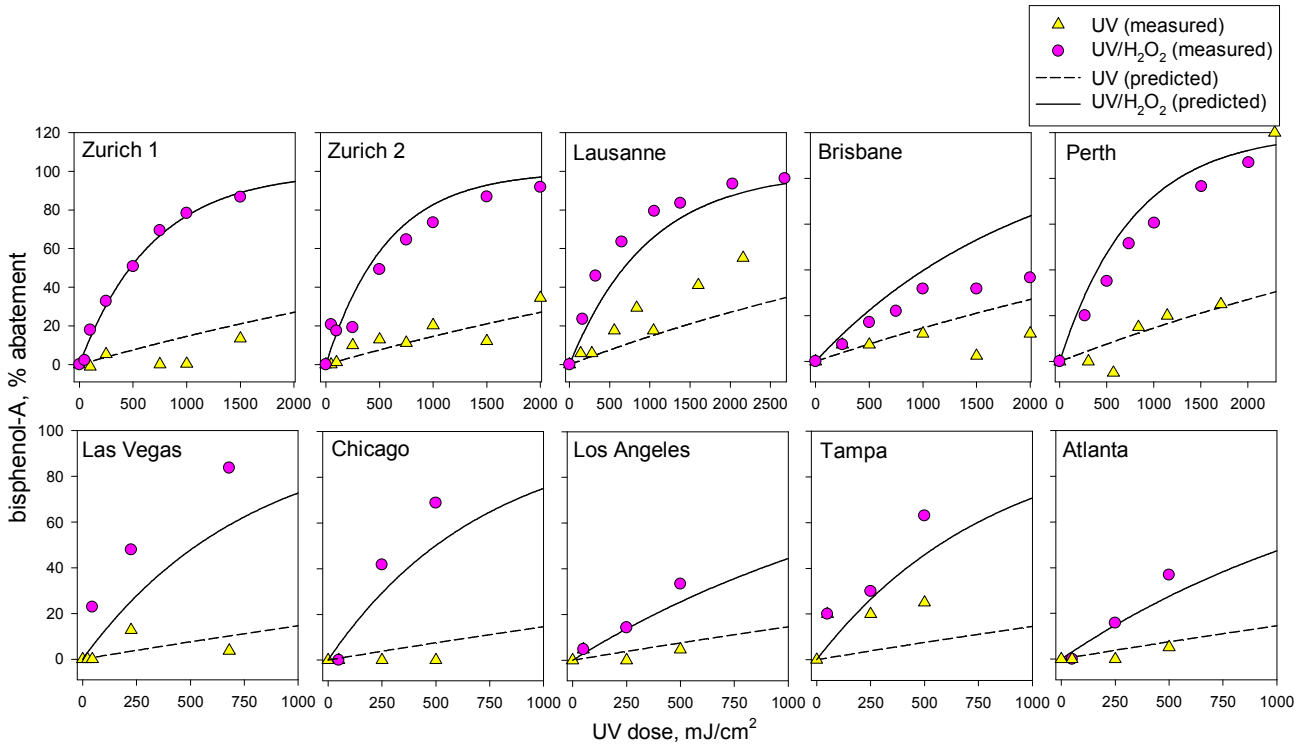

(j) carbamazepine

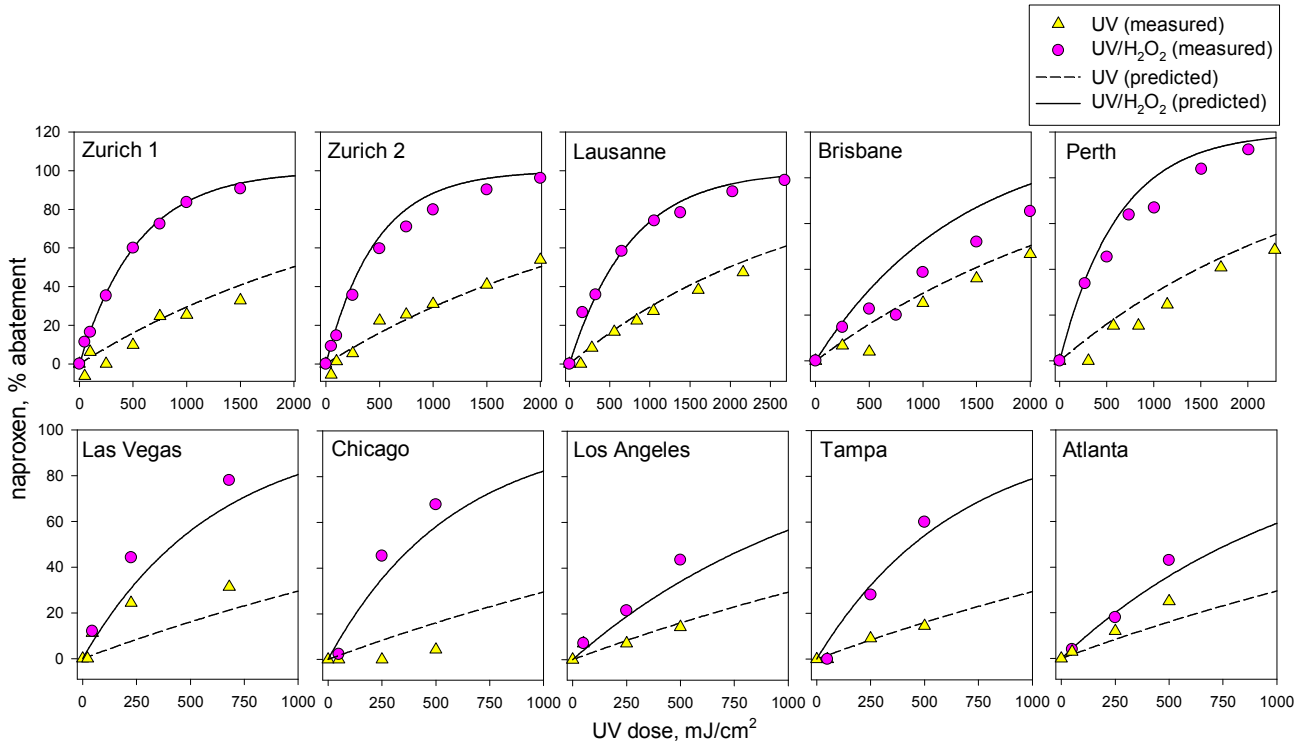

(k) primidone

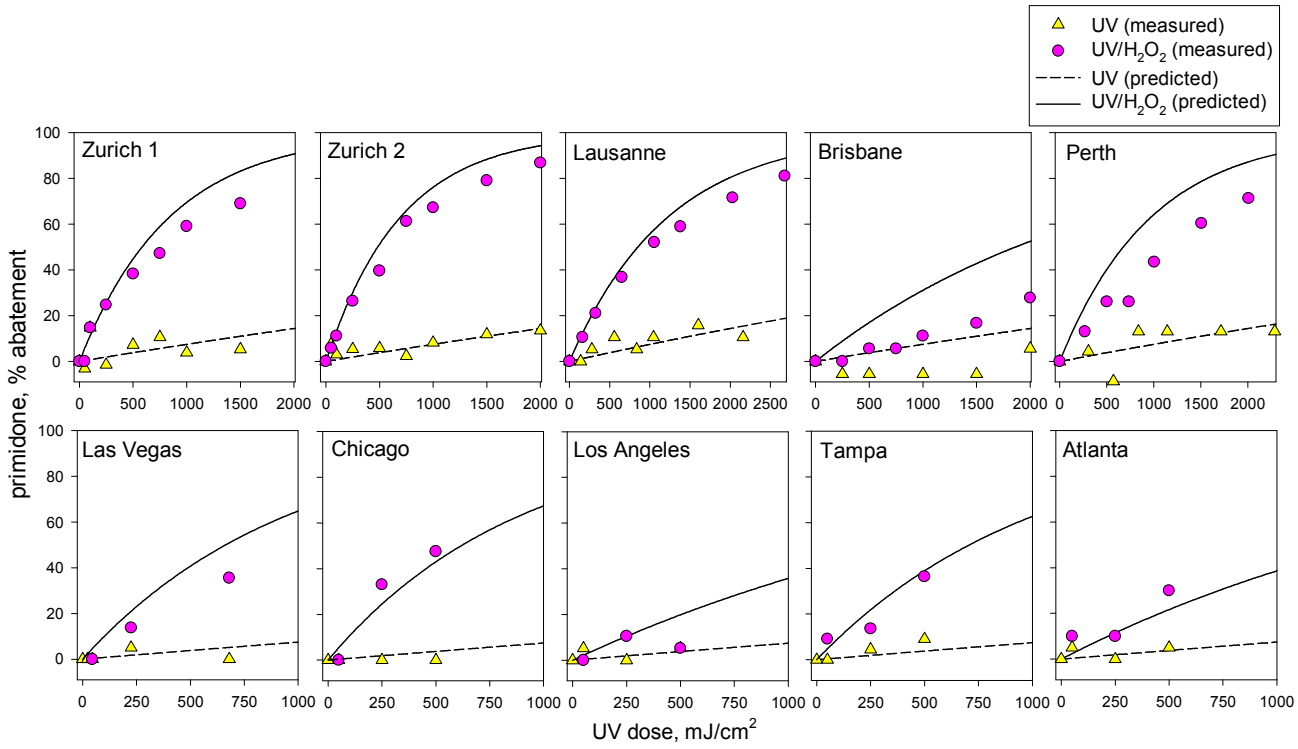

(l) atenolol

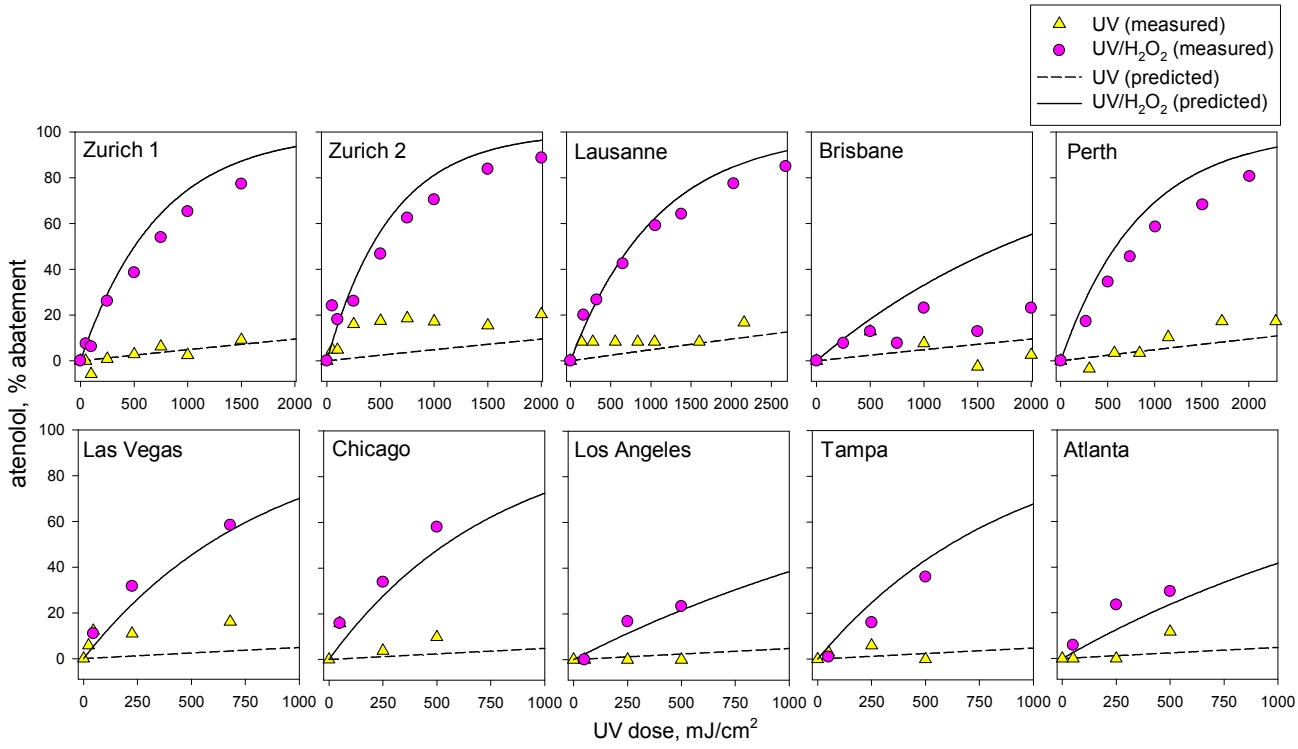

(m) trimethoprim

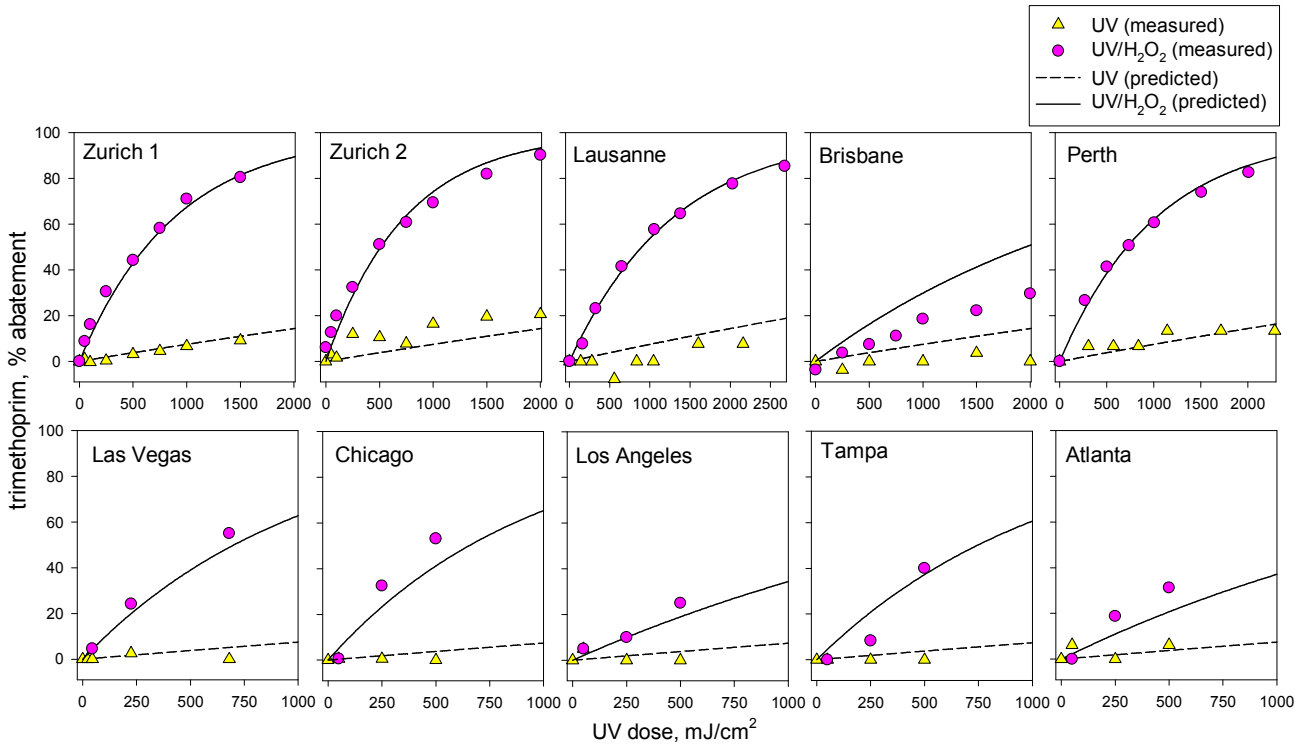

(n) gemfibrozil

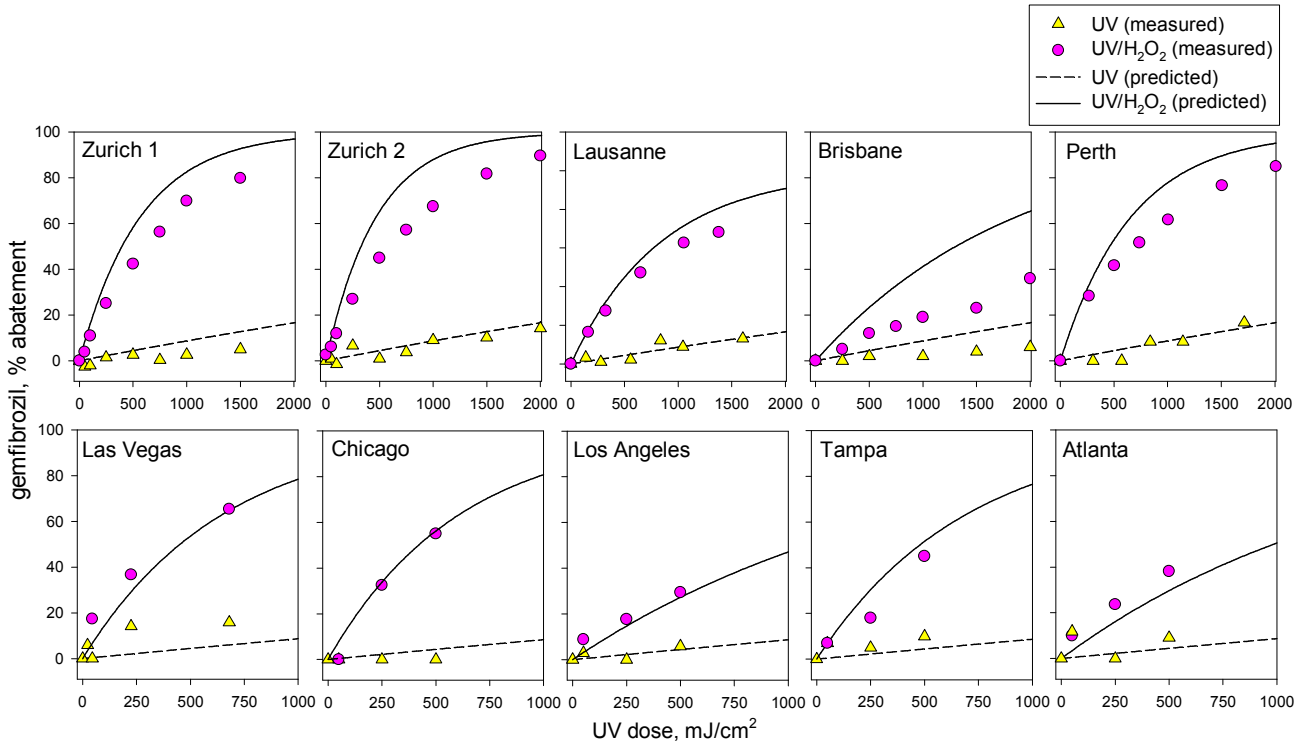

(o) DEET

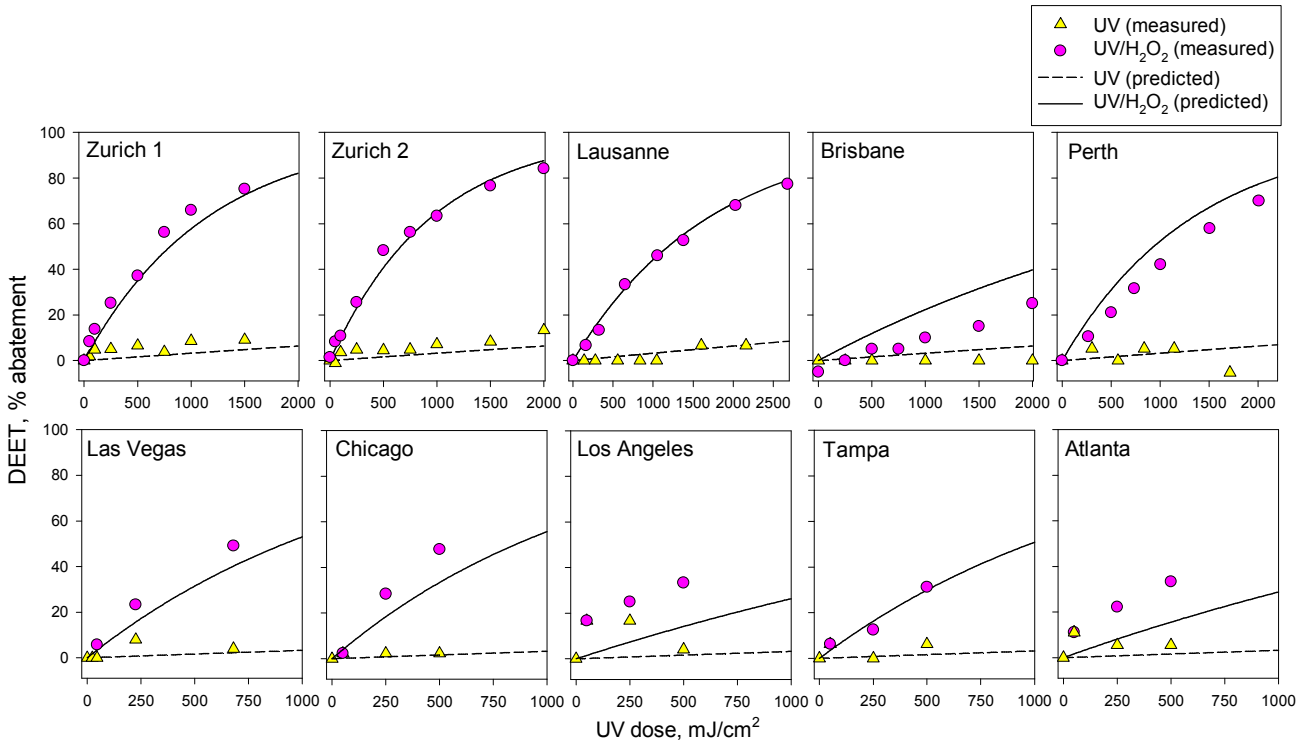

(p) meprobamate

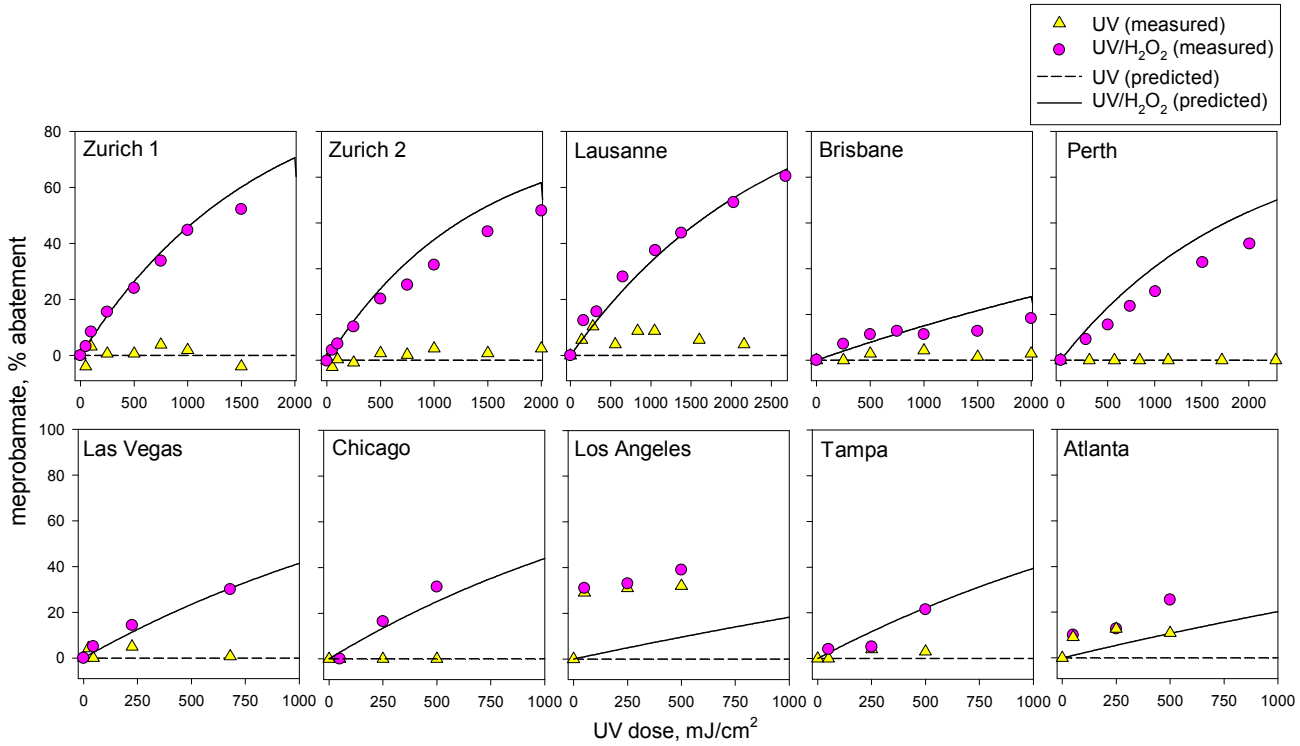

Figure S2. Plots of the logarithmic relative residual micropollutant concentration as a function of the UV dose during treatment of the wastewater effluents with UV (triangles and dashed lines) and UV/H_2O_2 (circles and solid lines) ($[H_2O_2]_0$ = 10 mg L^{-1}). Symbols and lines represent the measured and fitted data, respectively.

(a) diclofenac

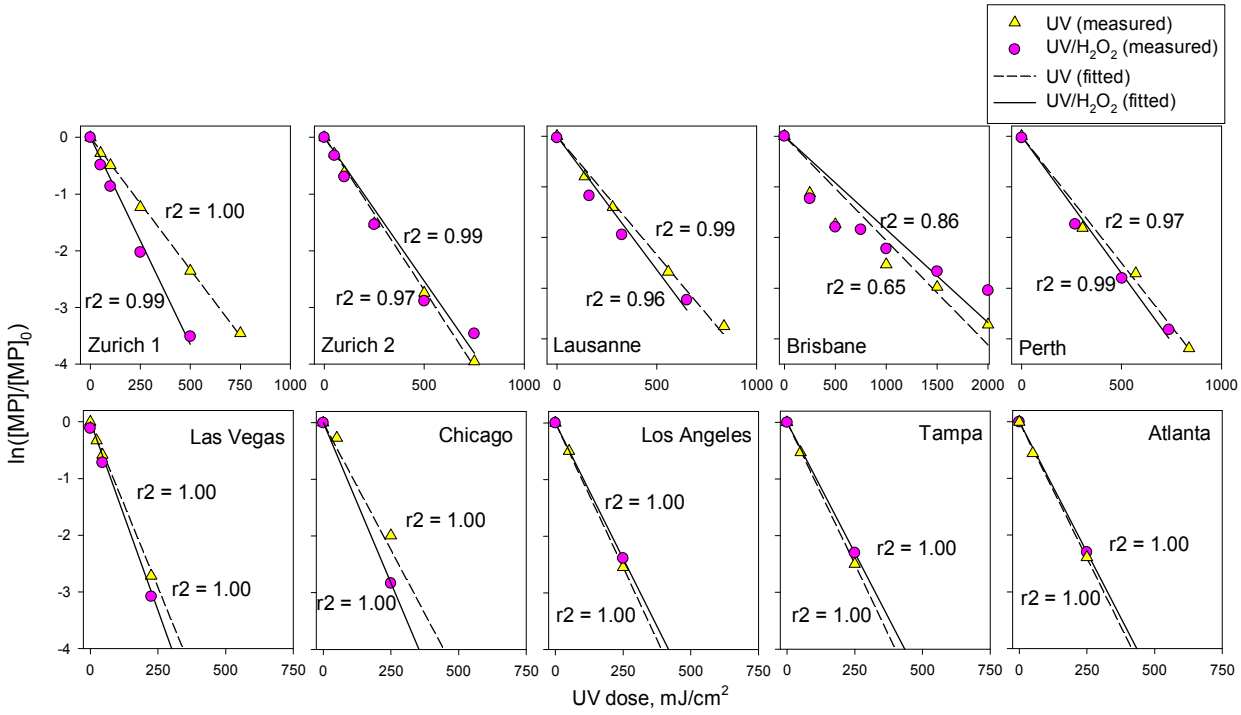

(b) NDMA

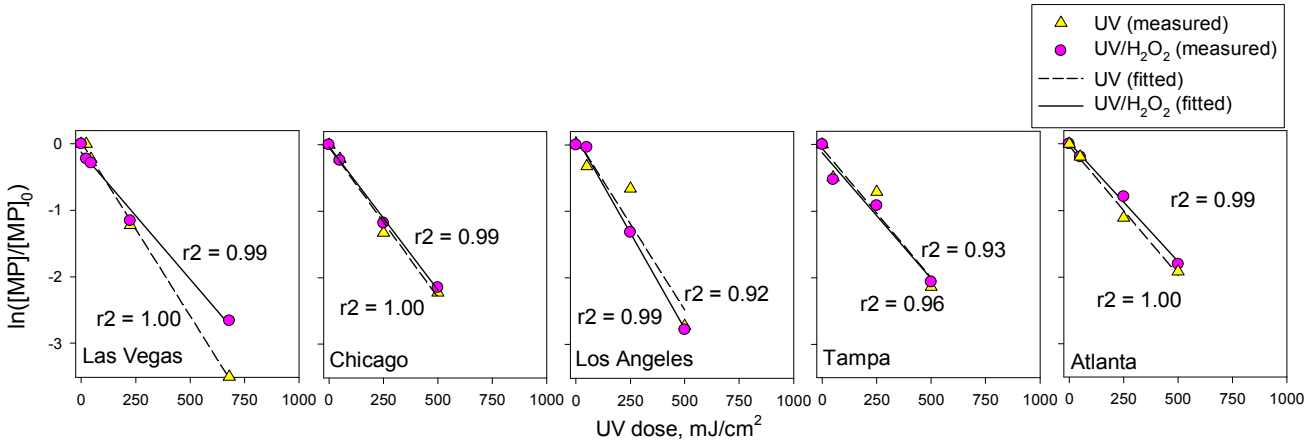

(c) triclosan

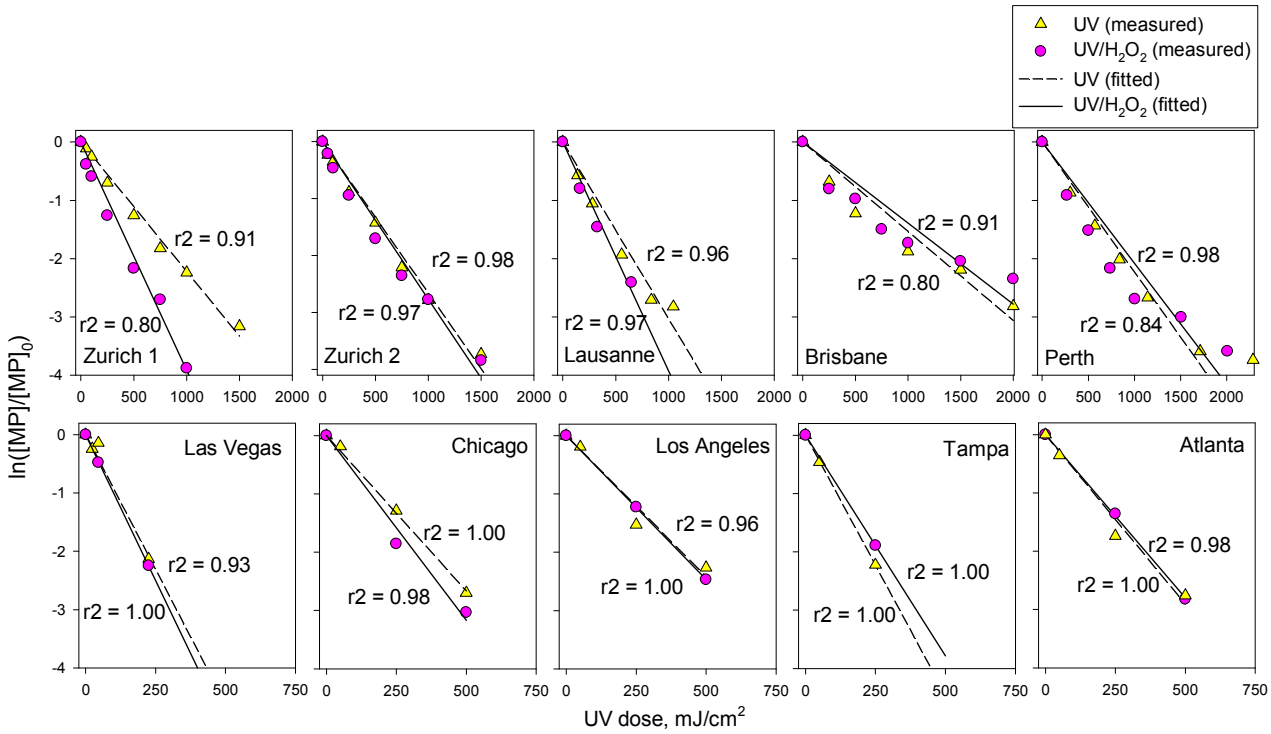

(d) sulfamethoxazole

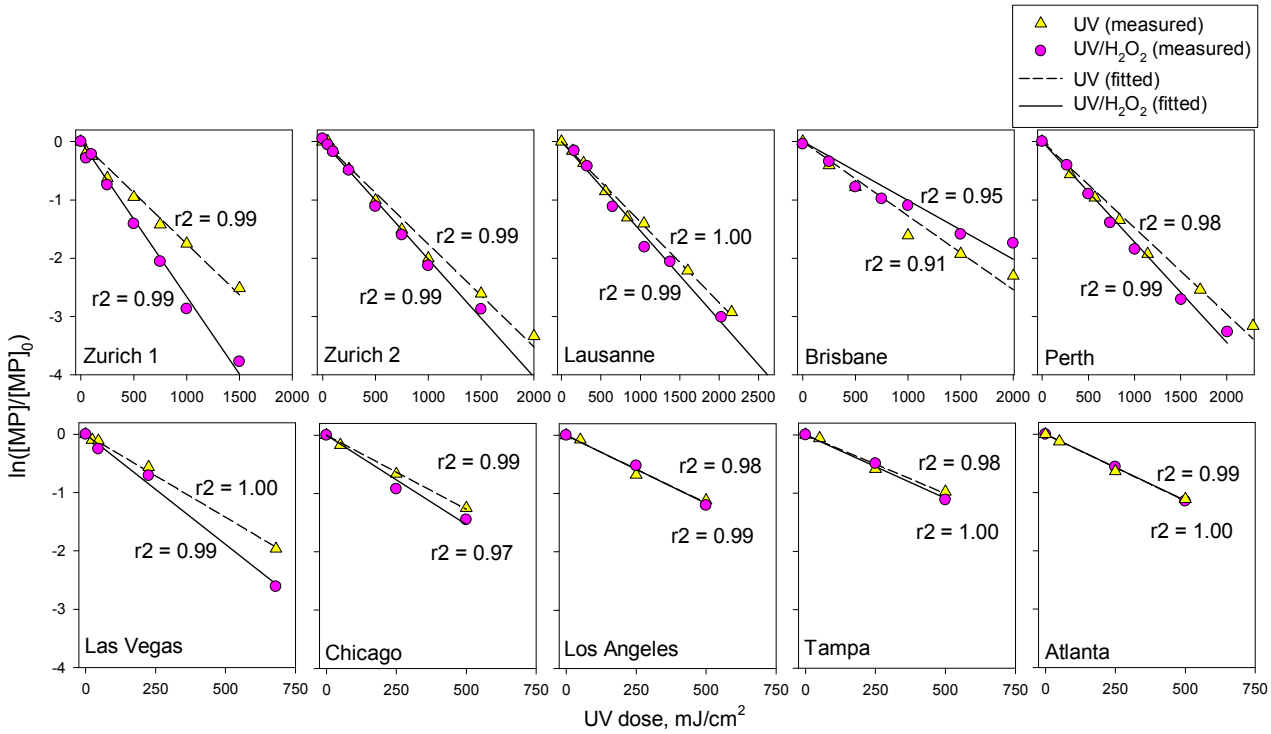

(e) phenytoin

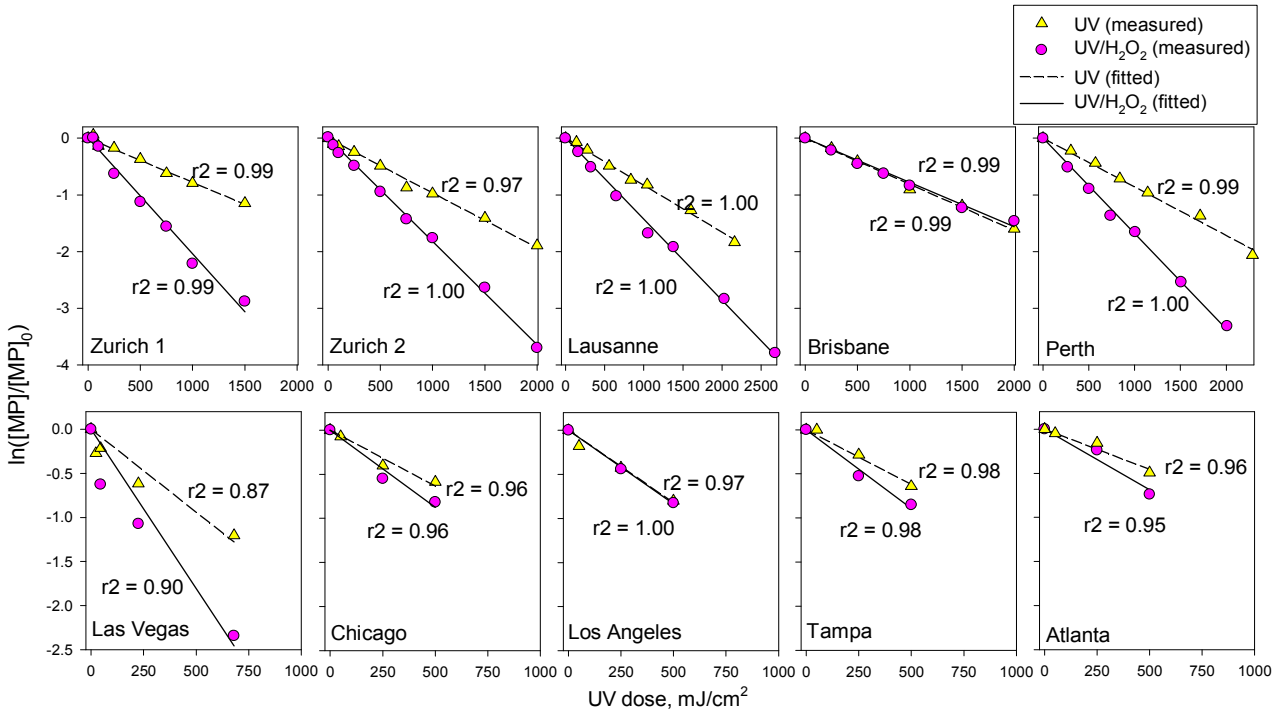

(f) atrazine

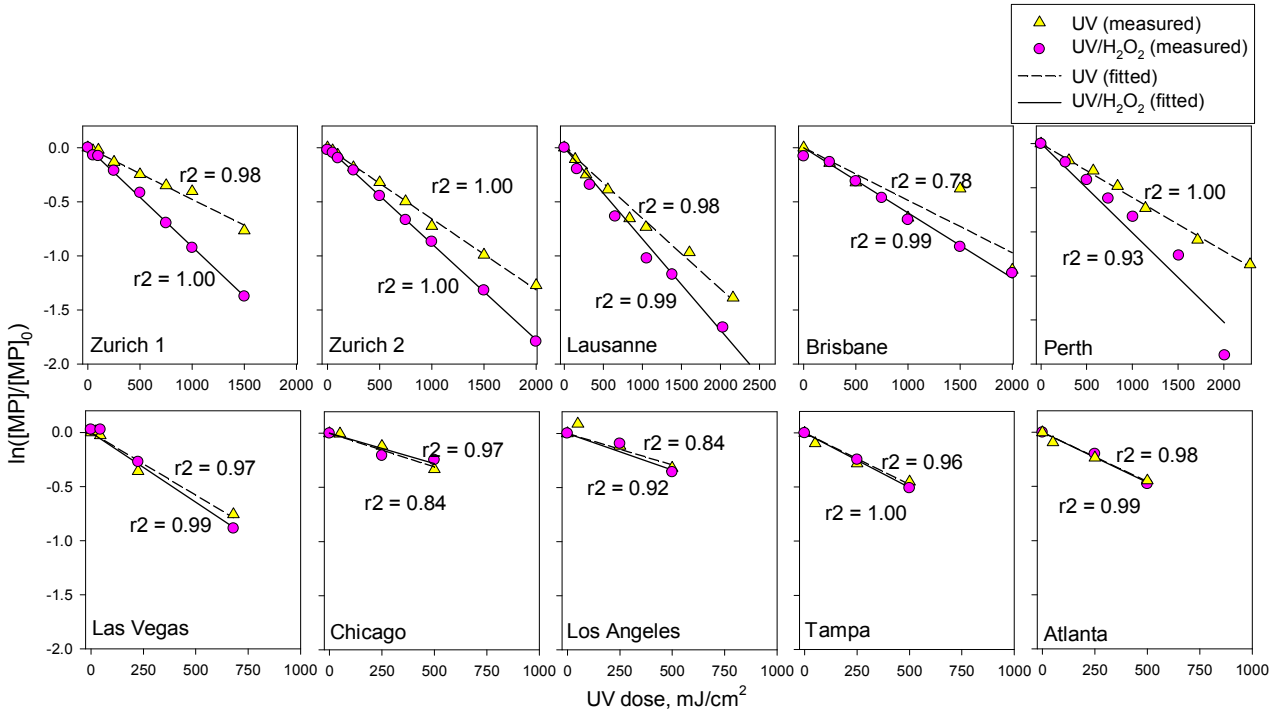

(g) naproxen

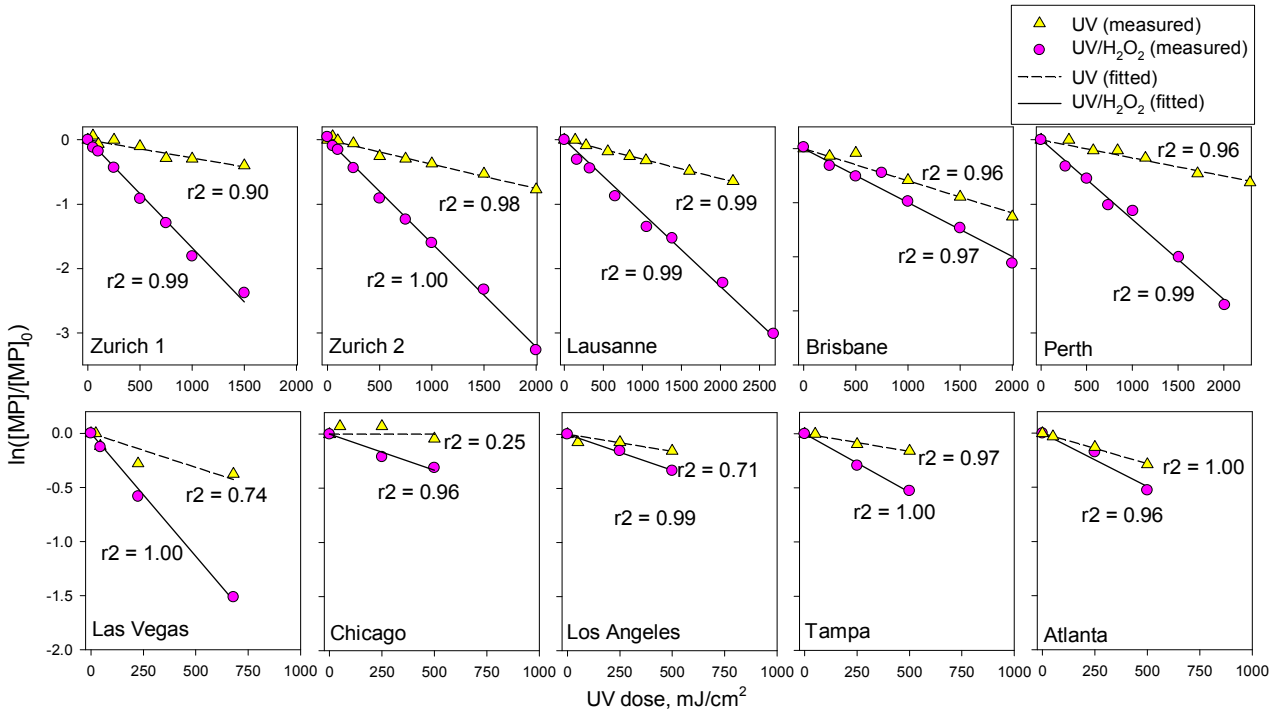

(h) ibuprofen

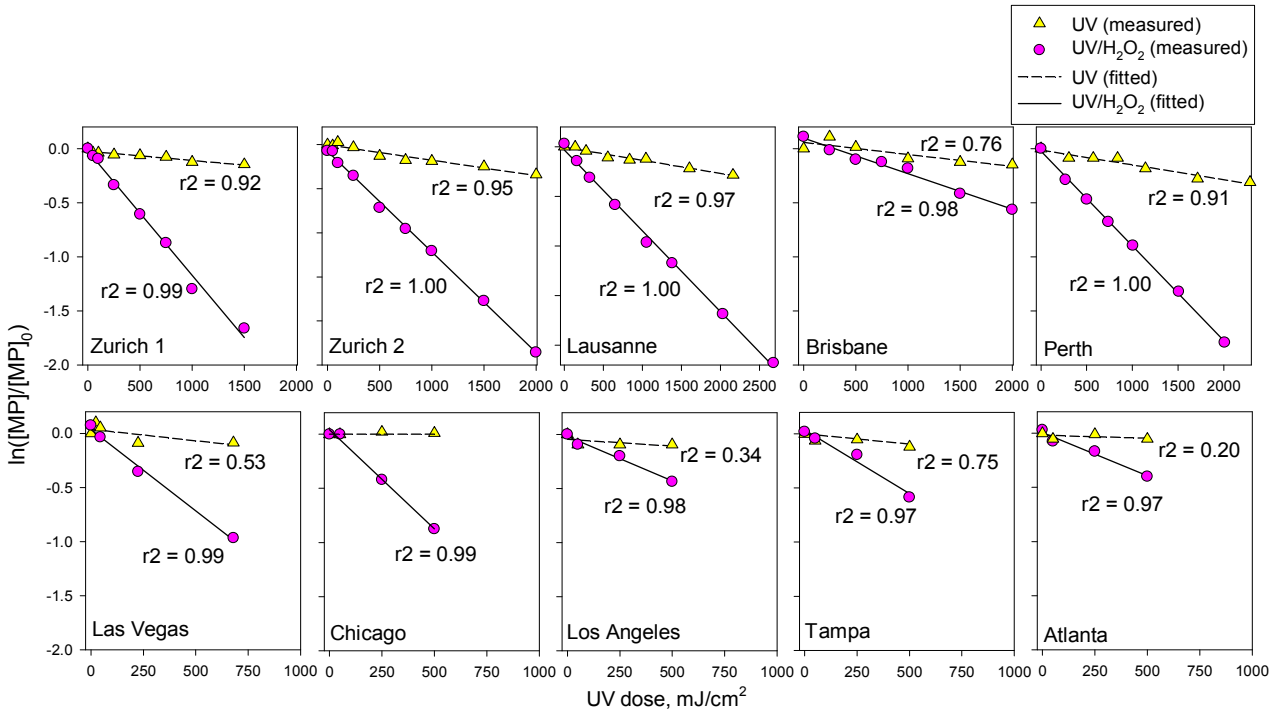

(i) bisphenol A

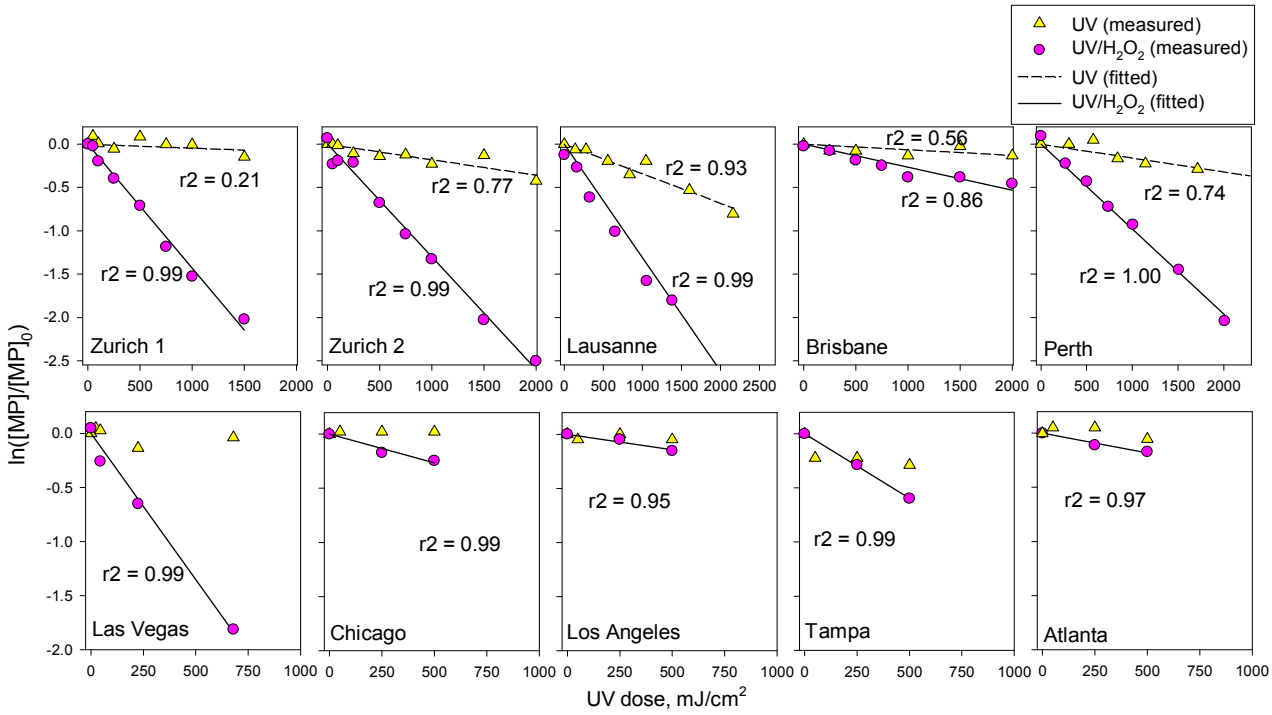

(j) carbamazepine

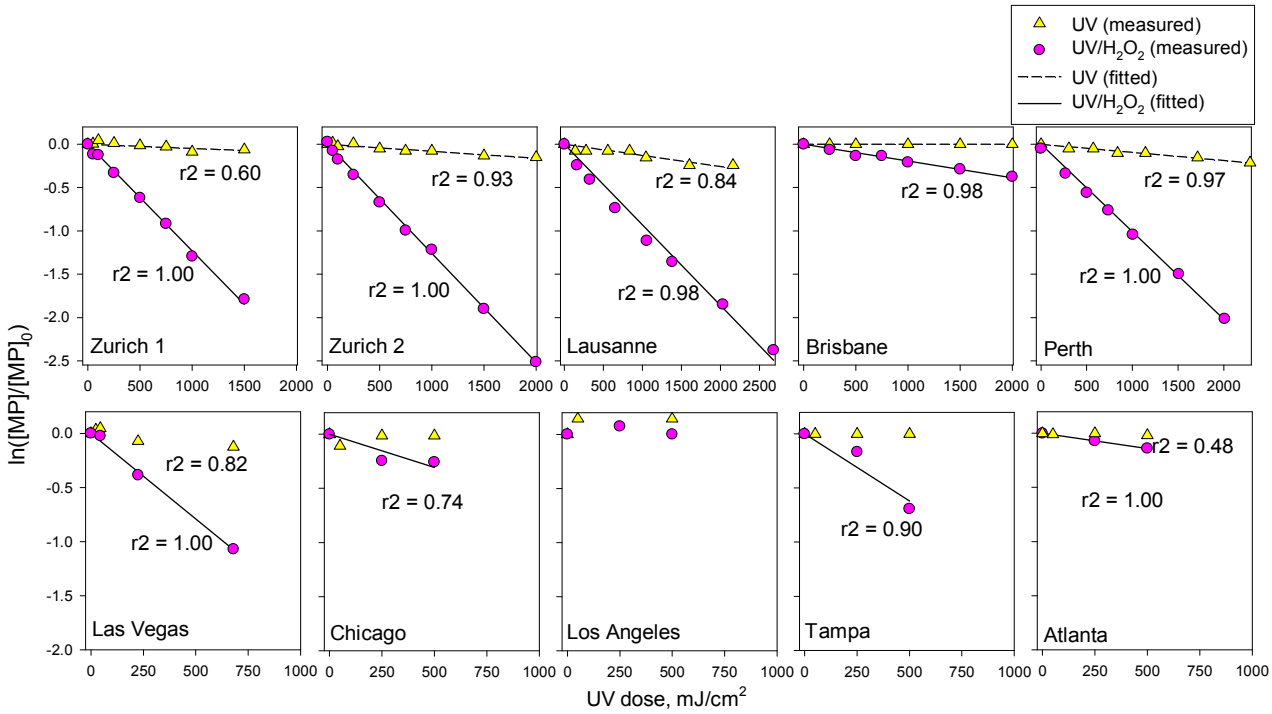

(k) primidone

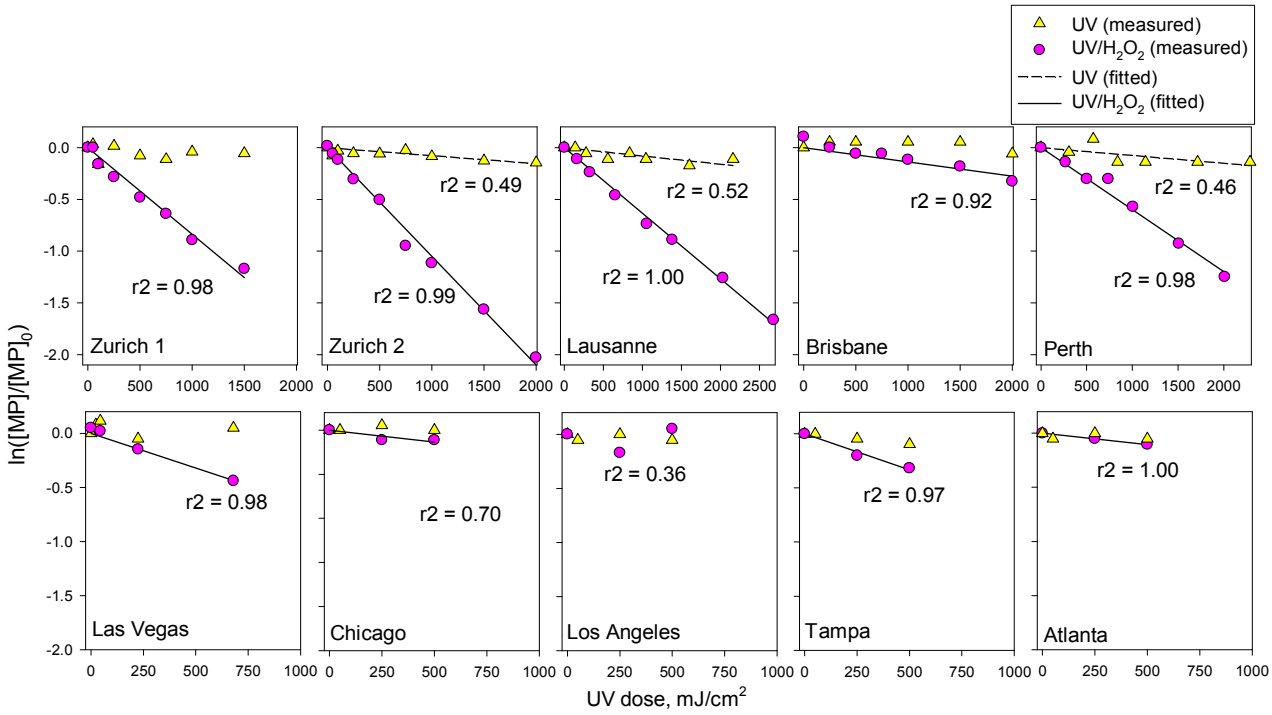

(l) atenolol

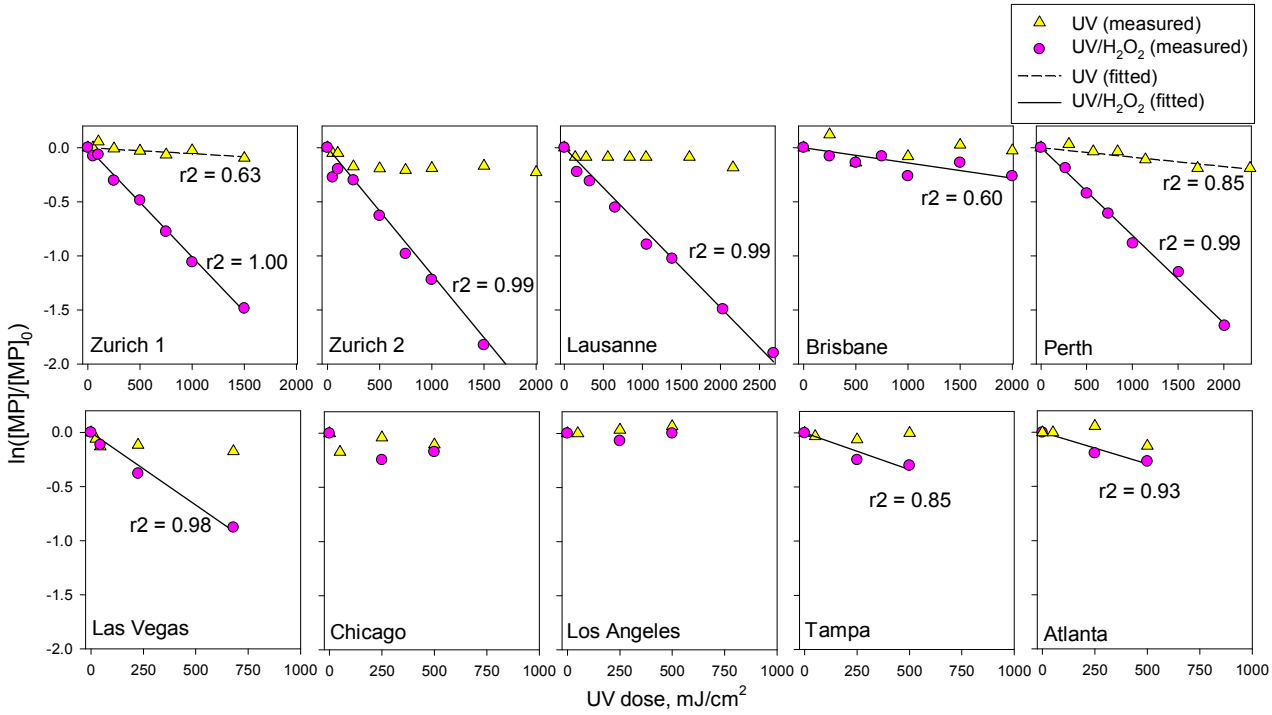

(m) trimethoprim

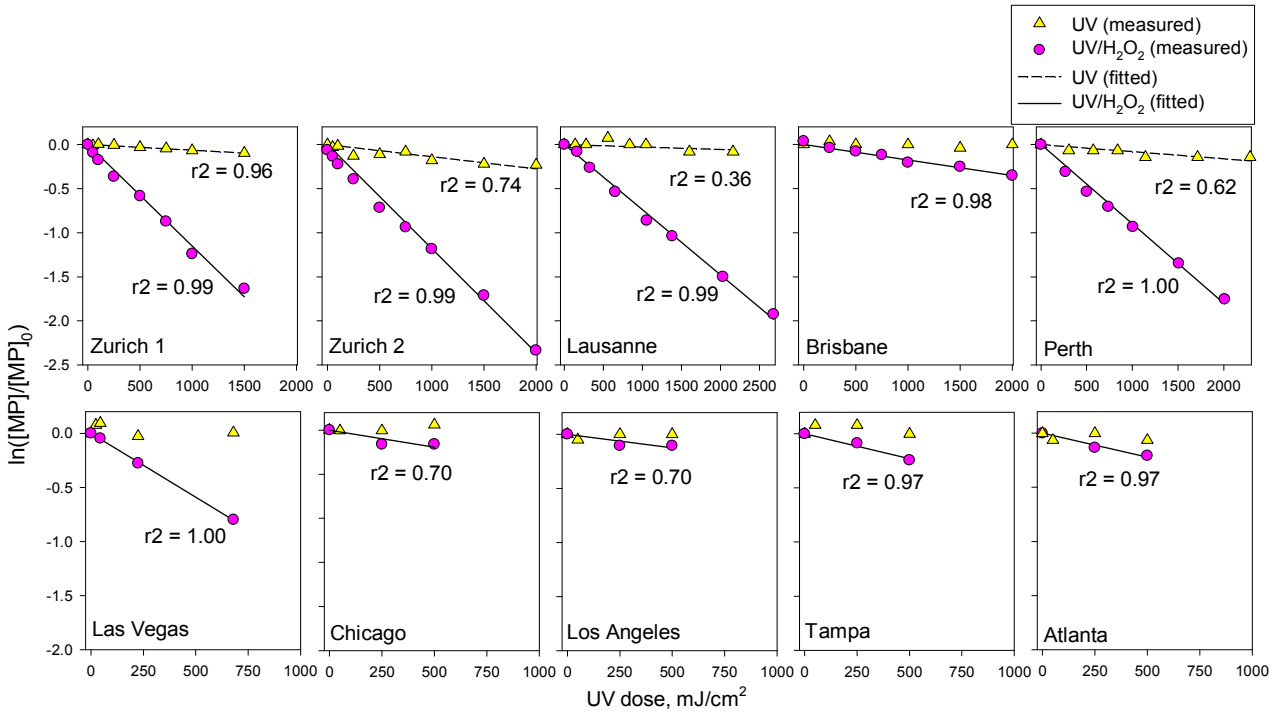

(n) gemfibrozil

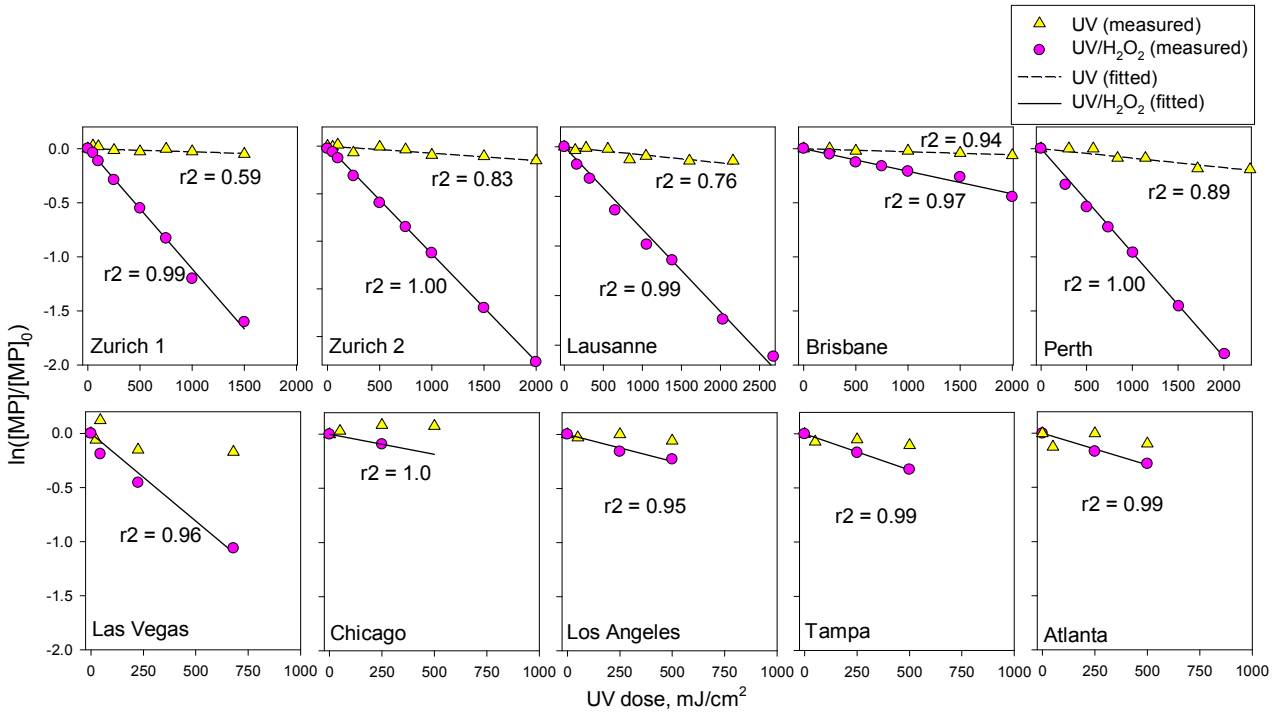

(o) DEET

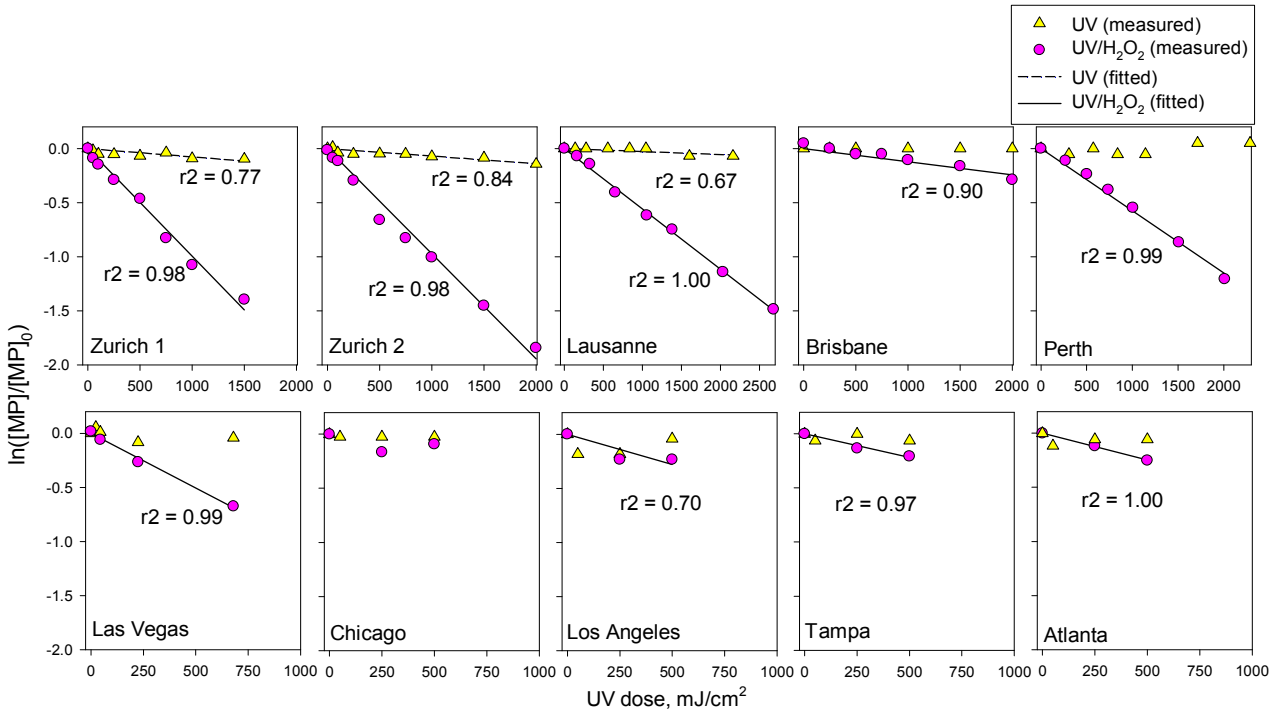

(p) meprobamate

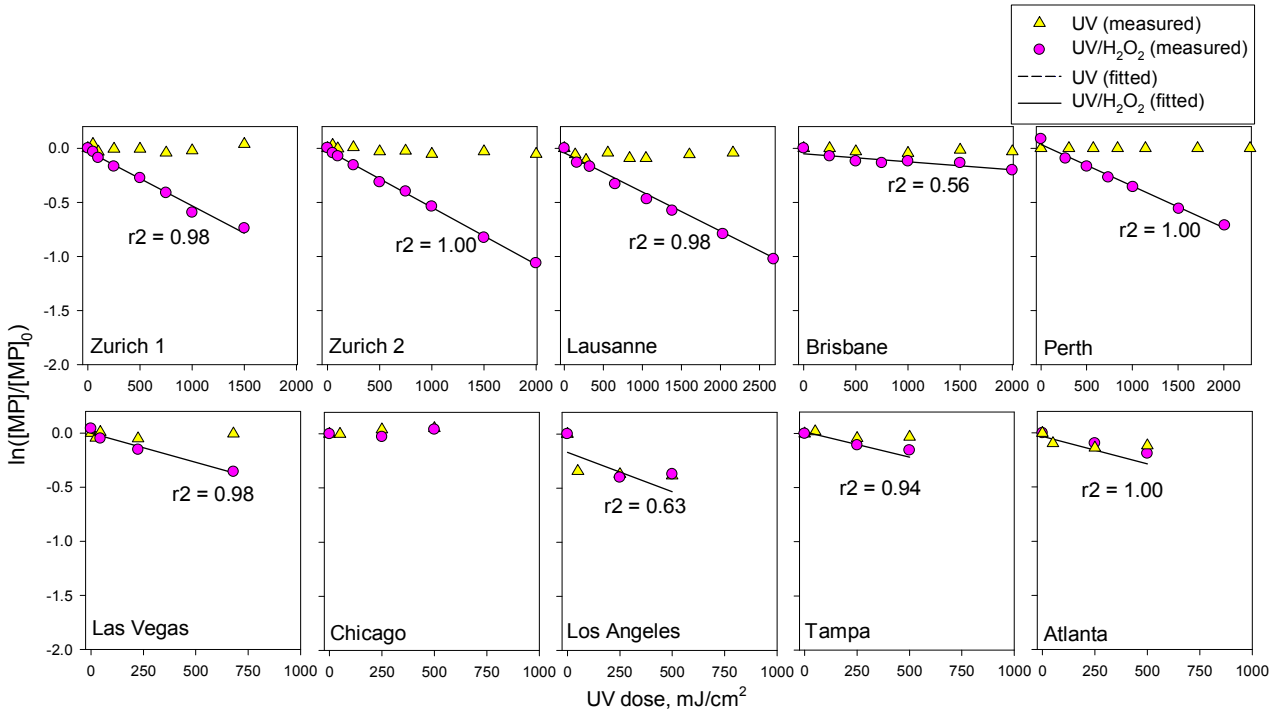

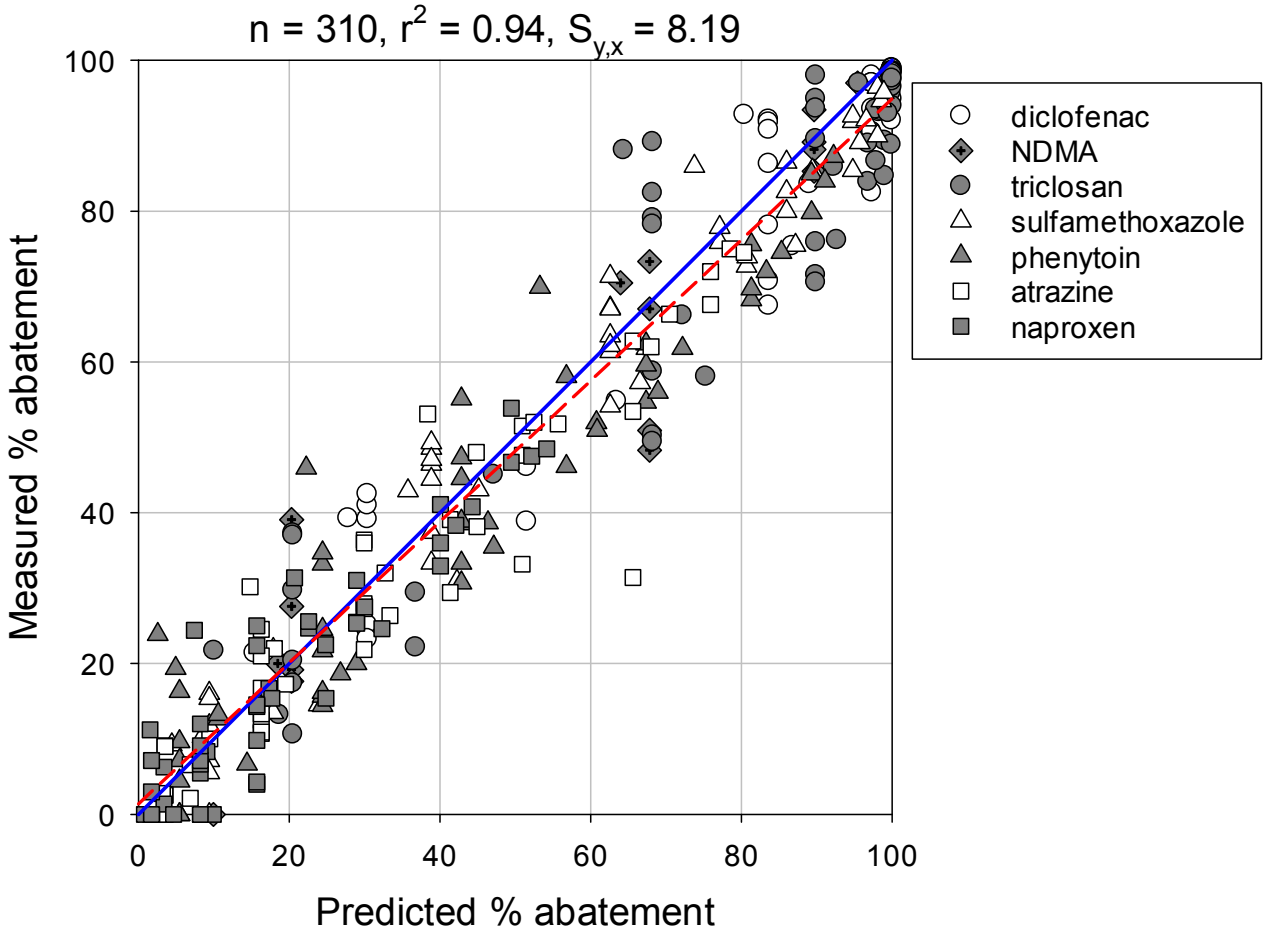

Figure S3. Measured and predicted % abatement of the group I and II micropollutants (Table 1) during UV treatment of wastewater effluents. The UV doses for the U.S. wastewater effluents were in the range of 0 – 750 mJ cm^{-2}, and 0 – 2700 mJ cm^{-2} for the other wastewater effluents. For modeling of the UV photolysis of micropollutants, empirical quantum yields ($\Phi_{MP\text{-}ww}$, Table 1) were used in all cases. The blue solid line indicates the one-to-one linear correlation of data, i.e., y = x, n = 310, r^2 = 0.94, and Sy,x = 8.19 in which n is the number of data points, r^2 and Sy,x represents the goodness of fit and standard errors of estimate, respectively. The Sy,x is calculated as $(SS/df)^{1/2}$ in which SS is the sum-of-squares of the distance of the linear correlation from the data points ($=\sum(Y' - Y)^2$) and df is the number of degrees of freedom of the fit (=310). The red dash line indicates the linear regression of data, i.e., y = 0.94*x+ 1.4, n = 310, r^2 = 0.95, and Sy,x = 7.67.

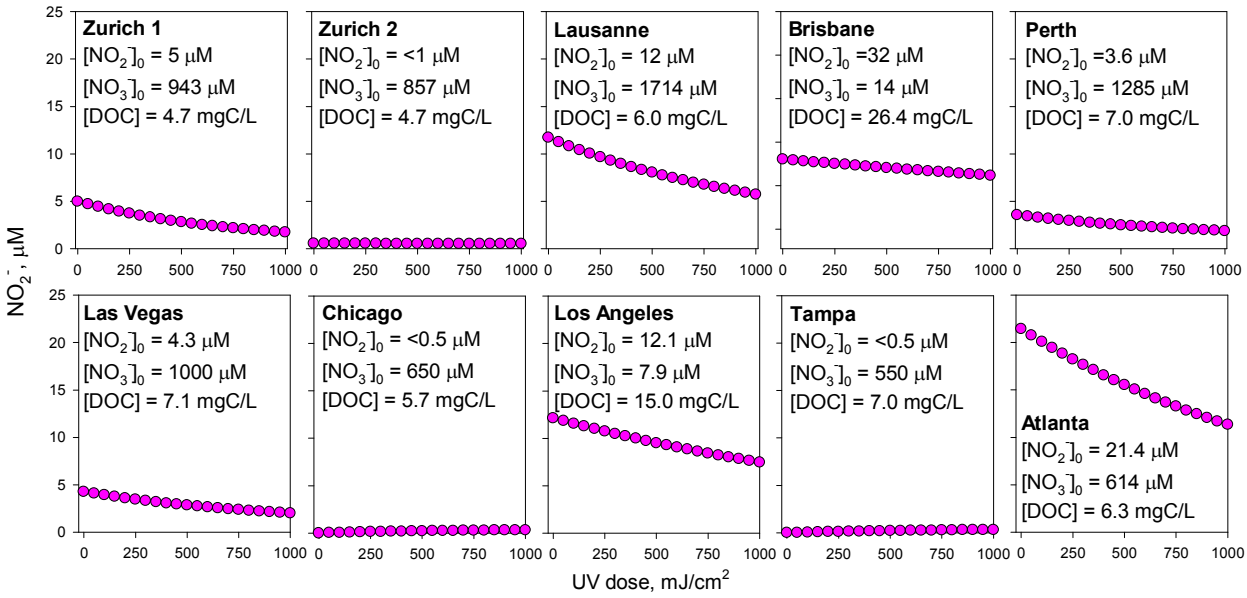

Figure S4. Simulated concentration of NO_2^- during UV/H_2O_2 treatment of the wastewater effluents. See Text-S5 for discussion.

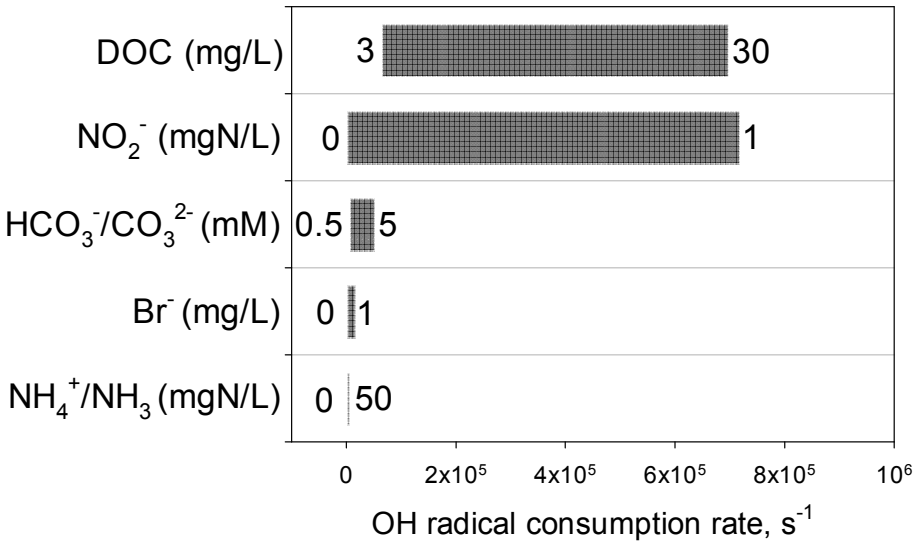

Figure S5. Ranges of the •OH consumption rate at pH 7 by each of water matrix component such as DOC, nitrite, carbonate species, bromide and ammonia species during UV/H_2O_2 treatment of municipal wastewater effluent. The •OH consumption rate was calculated by $k_{\bullet OH,Si}[S_i]$ in which $k_{\bullet OH,Si}$ is the second-order rate constant for the reaction of •OH and $[S_i]$ is the concentration of the matrix components. The numbers at each side of the bars indicate the typical concentration ranges of the selected water matrix components. See Text-S6 for discussion.

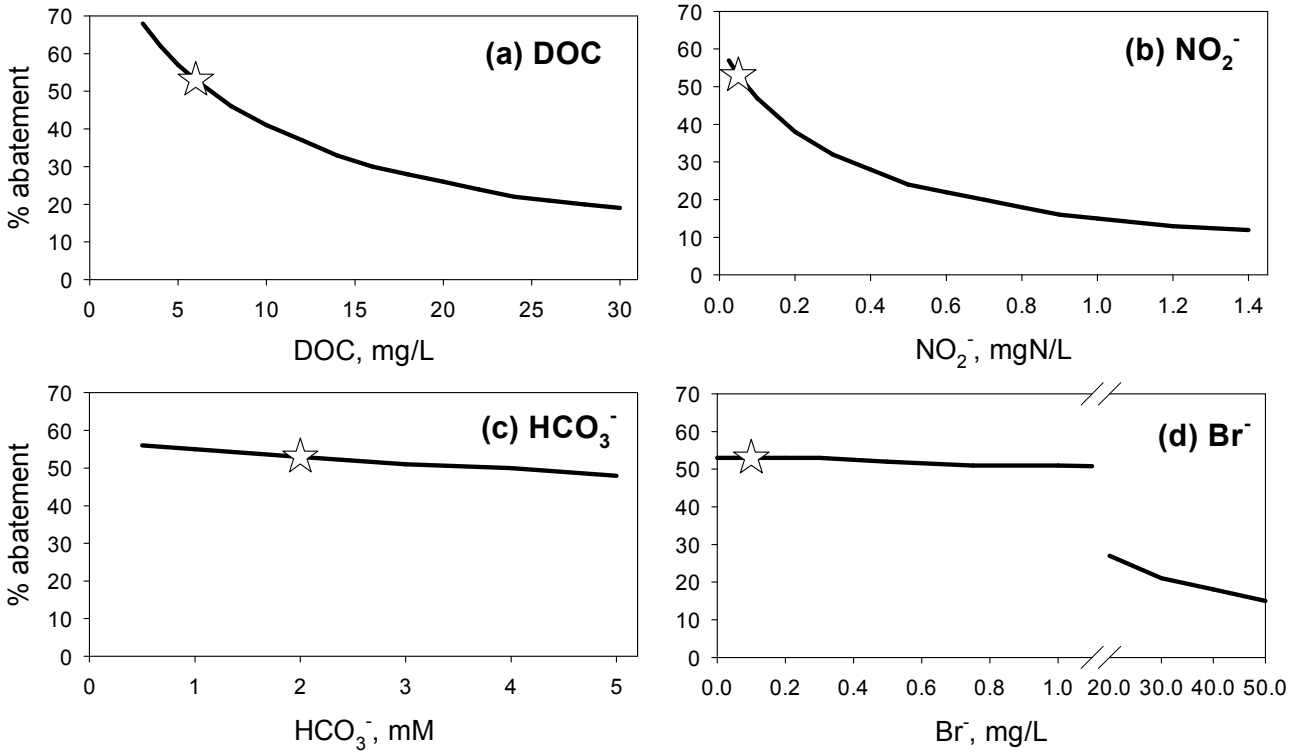

Figure S6. Calculated % abatement levels of a micropollutant during UV/H_2O_2 treatment of a hypothetical wastewater effluent ([DOC] = 3 mg/L, [NO_2^-] = 0.05 mgN/L, [HCO_3^-/CO_3^{2-}] = 2 mM, [Br^-] = 0.1 mg/L and pH 7) with varying concentration of (a) DOC (3 – 30 mg/L), (b) NO_2^- (0 – 1 mgN/L), (c) HCO_3^-/CO_3^{2-} (0.5 – 5 mM), and (d) Br^- (0 – 50 mg/L). The selected hypothetical micropollutant is eliminated only by its reaction with •OH with a second-order rate constant of 10^{10} M^{-1} s^{-1}. The applied UV and H_2O_2 doses were 1000 mJ/cm^2 and 10 mg/L, respectively. The % abatement levels were calculated by using Eqs. 2 and 3 in the main text. See Text-S6 for discussion.

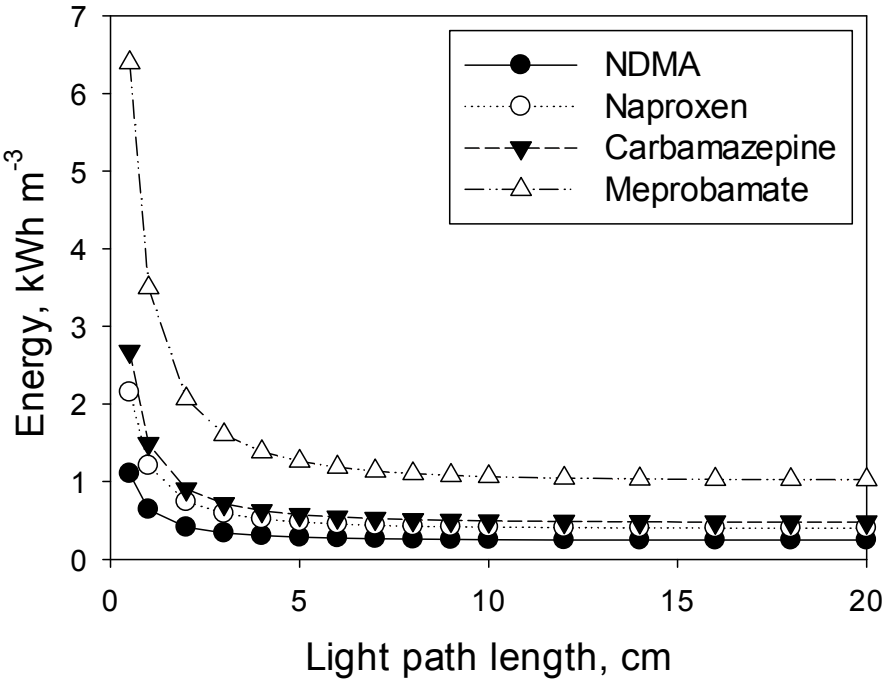

Figure S7. Energy requirements in kWh/m^3 for 90% abatement of the selected micropollutants (NDMA, naproxen, carbamazepine, and meprobamate) by UV/H_2O_2 ($[H_2O_2]_0$ = 10 mg L^{-1}) in a hypothetical wastewater effluent as a function of the light path length ([DOC] = 6 mg L^{-1}, A_{254nm} (cm^{-1}) = ε_{DOC}[DOC] + $\varepsilon_{H2O2}[H_2O_2]_0$, ε_{DOC} = 0.022 $(mgC/L)^{-1}$ cm^{-1} and ε_{H2O2} = 19.6 M^{-1} cm^{-1}, total carbonate = 2 mM, and pH = 7).

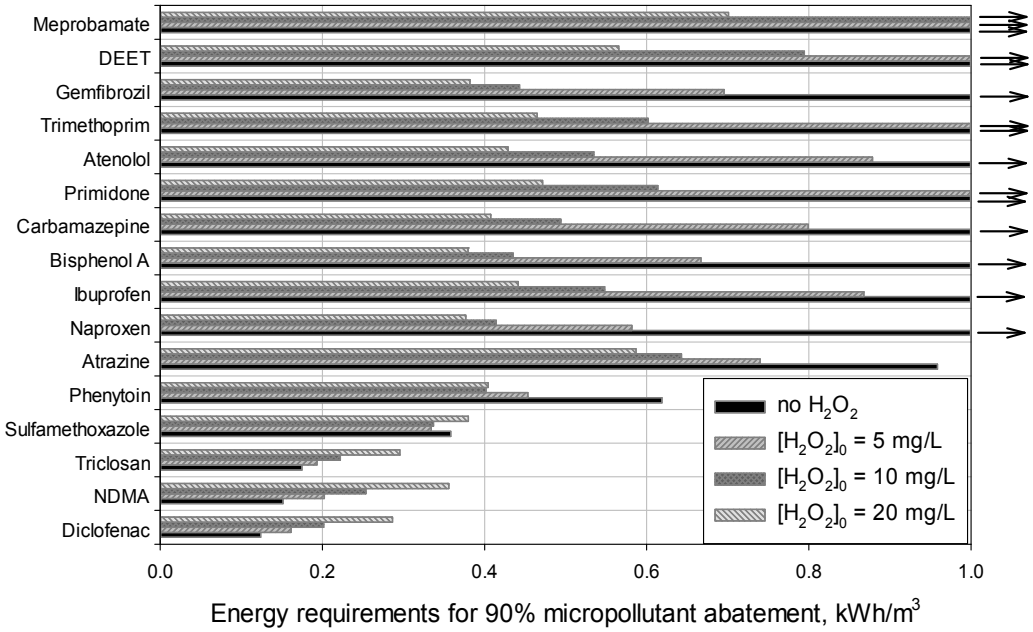

Compounds	No H_2O_2	$[H_2O_2]_0$ = 5 mg L^{-1}	$[H_2O_2]_0$ = 10 mg L^{-1}	$[H_2O_2]_0$ = 20 mg L^{-1}
Diclofenac	0.12	0.16	0.20	0.29
NDMA	0.15	0.20	0.25	0.36
Triclosan	0.17	0.19	0.22	0.30
Sulfamethoxazole	0.36	0.33	0.34	0.38
Phenytoin	0.62	0.45	0.40	0.40
Atrazine	0.96	0.74	0.64	0.59
Naproxen	1.89	0.58	0.41	0.38
Ibuprofen	5.67	0.87	0.55	0.44
Bisphenol A	4.86	0.67	0.44	0.38
Carbamazepine	11.35	0.80	0.49	0.41
Primidone	11.94	1.02	0.61	0.47
Atenolol	13.61	0.88	0.53	0.43
Trimethoprim	13.89	1.00	0.60	0.46
Gemfibrozil	7.48	0.70	0.44	0.38
DEET	20.63	1.37	0.79	0.57
Meprobamate	136.14	1.93	1.06	0.70

Figure S8. Energy requirements in kWh/m^3 for 90% abatement of the selected micropollutants by UV and UV/H_2O_2 in a hypothetical wastewater effluent ([DOC] = 6 mg L^{-1}, A_{254nm} (cm^{-1}) = ε_{DOC}[DOC] + $\varepsilon_{H2O2}[H_2O_2]_0$, ε_{DOC} = 0.022 $(mgC/L)^{-1}$ cm^{-1} and ε_{H2O2} = 19.6 M^{-1} cm^{-1}, total carbonate = 2 mM, and pH = 7). An optical path length of 10 cm was applied. The arrows indicate an energy requirement of more than 1 kWh/m^3.

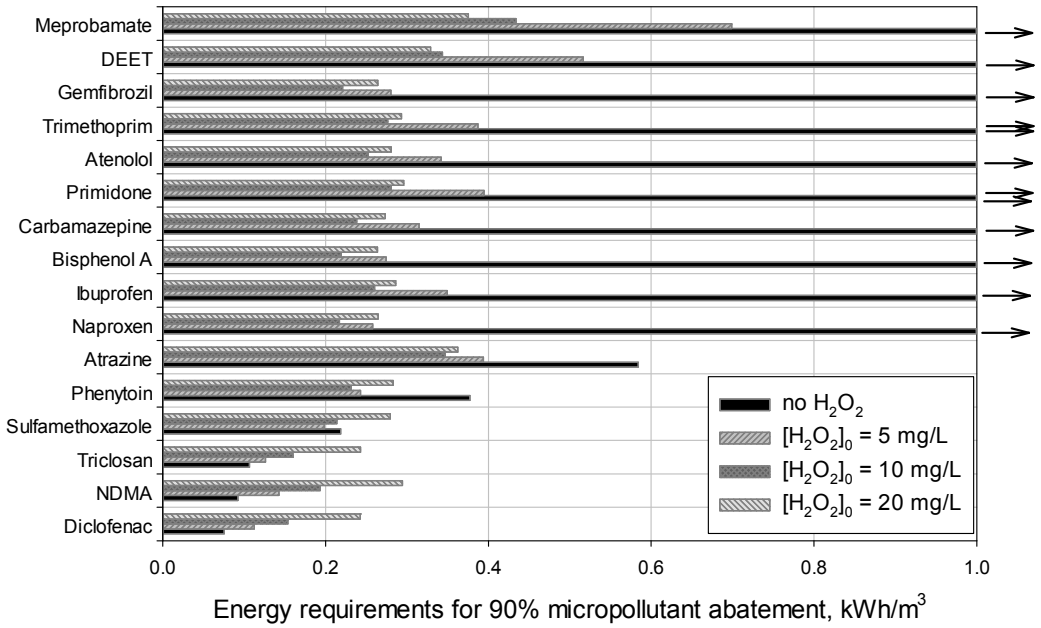

Compounds	No H_2O_2	$[H_2O_2]_0$ = 5 mg L^{-1}	$[H_2O_2]_0$ = 10 mg L^{-1}	$[H_2O_2]_0$ = 20 mg L^{-1}
Diclofenac	0.08	0.11	0.15	0.24
NDMA	0.09	0.14	0.19	0.29
Triclosan	0.11	0.13	0.16	0.24
Sulfamethoxazole	0.22	0.20	0.21	0.28
Phenytoin	0.38	0.24	0.23	0.28
Atrazine	0.58	0.39	0.35	0.36
Naproxen	1.15	0.26	0.22	0.26
Ibuprofen	3.46	0.35	0.26	0.29
Bisphenol A	2.96	0.27	0.22	0.26
Carbamazepine	6.91	0.31	0.24	0.27
Primidone	7.28	0.39	0.28	0.30
Atenolol	8.30	0.34	0.25	0.28
Trimethoprim	8.47	0.39	0.28	0.29
Gemfibrozil	4.56	0.28	0.22	0.26
DEET	12.57	0.52	0.34	0.33
Meprobamate	82.96	0.70	0.43	0.38

Figure S9. Energy requirements in kWh m^{-3} for 90% abatement of the selected micropollutants by UV and UV/H_2O_2 in a hypothetical wastewater effluent ([DOC] = 3 mg L^{-1} A_{254nm} (cm^{-1}) = ε_{DOC}[DOC] + $\varepsilon_{H2O2}[H_2O_2]_0$, ε_{DOC} = 0.022 $(mgC/L)^{-1}$ cm^{-1} and ε_{H2O2} = 19.6 M^{-1} cm^{-1}, total carbonate = 2 mM, and pH = 7). An optical path length of 10 cm was applied. The arrows indicate an energy requirement of more than 1 kWh/m^3.

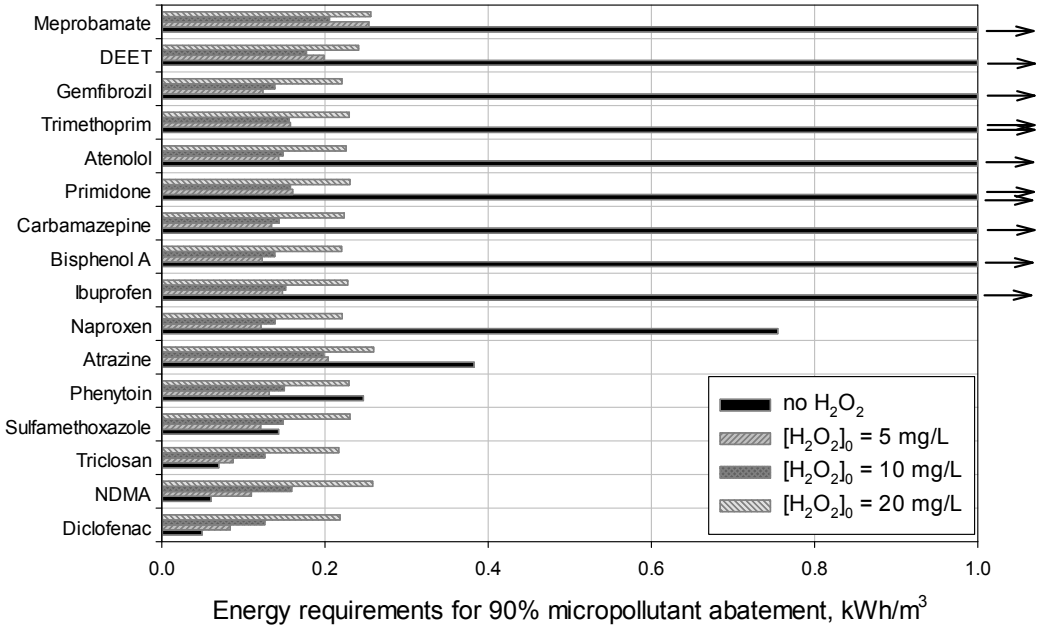

Compounds	No H_2O_2	$[H_2O_2]_0$ = 5 mg L^{-1}	$[H_2O_2]_0$ = 10 mg L^{-1}	$[H_2O_2]_0$ = 20 mg L^{-1}
Diclofenac	0.05	0.08	0.13	0.22
NDMA	0.06	0.11	0.16	0.26
Triclosan	0.07	0.09	0.13	0.22
Sulfamethoxazole	0.14	0.12	0.15	0.23
Phenytoin	0.25	0.13	0.15	0.23
Atrazine	0.38	0.20	0.20	0.26
Naproxen	0.75	0.12	0.14	0.22
Ibuprofen	2.26	0.15	0.15	0.23
Bisphenol A	1.94	0.12	0.14	0.22
Carbamazepine	4.53	0.13	0.14	0.22
Primidone	4.77	0.16	0.16	0.23
Atenolol	5.44	0.14	0.15	0.23
Trimethoprim	5.55	0.16	0.16	0.23
Gemfibrozil	2.99	0.12	0.14	0.22
DEET	8.24	0.20	0.18	0.24
Meprobamate	54.36	0.25	0.21	0.26

Figure S10. Energy requirements in kWh m^{-3} for 90% abatement of the selected micropollutants by UV and UV/H_2O_2 in a hypothetical drinking water matrix ([DOC] = 1 mg L^{-1} A_{254nm} (cm^{-1}) = ε_{DOC}[DOC] + $\varepsilon_{H2O2}[H_2O_2]_0$, ε_{DOC} = 0.022 (mgC/L)$^{-1}$ cm^{-1} and ε_{H2O2} = 19.6 M^{-1} cm^{-1}, total carbonate = 2 mM, and pH = 7). An optical path length of 10 cm was applied. The arrows indicate an energy requirement of more than 1 kWh/m^3.

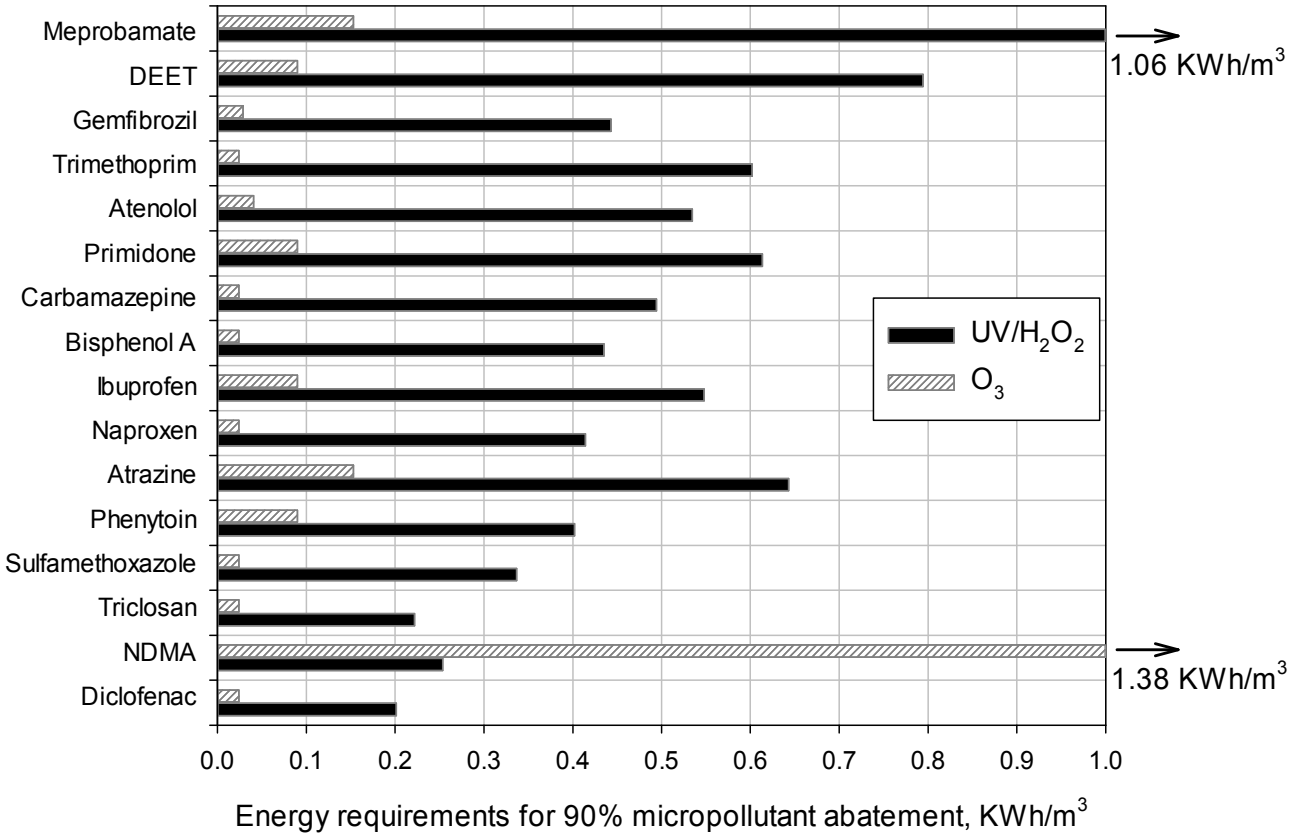

Figure S11. Energy requirements in kWh/m^3 for 90% abatement [i.e., electrical energy per order of magnitude (EEO)] of the selected micropollutants by ozonation and UV/H_2O_2 in hypothetical wastewater effluents with DOC of 6 mgC/L. For ozonation, complete ozone consumption was assumed. For UV/H_2O_2, an initial H_2O_2 concentration of 10 mg/L and an optical path length of 10 cm were applied. The absorption at 254nm (cm^{-1}) of the wastewater effluent is assumed to be $\varepsilon_{DOC}[DOC] + \varepsilon_{H2O2}[H_2O_2]_0$ and ε_{DOC} = 0.022 (mgC/L)$^{-1}$ cm^{-1} and ε_{H2O2} = 19.6 M^{-1} cm^{-1}. The pH of the wastewater effluent is 7 with 2 mM of carbonate. The arrows indicate an energy requirement of more than 1 kWh/m^3.

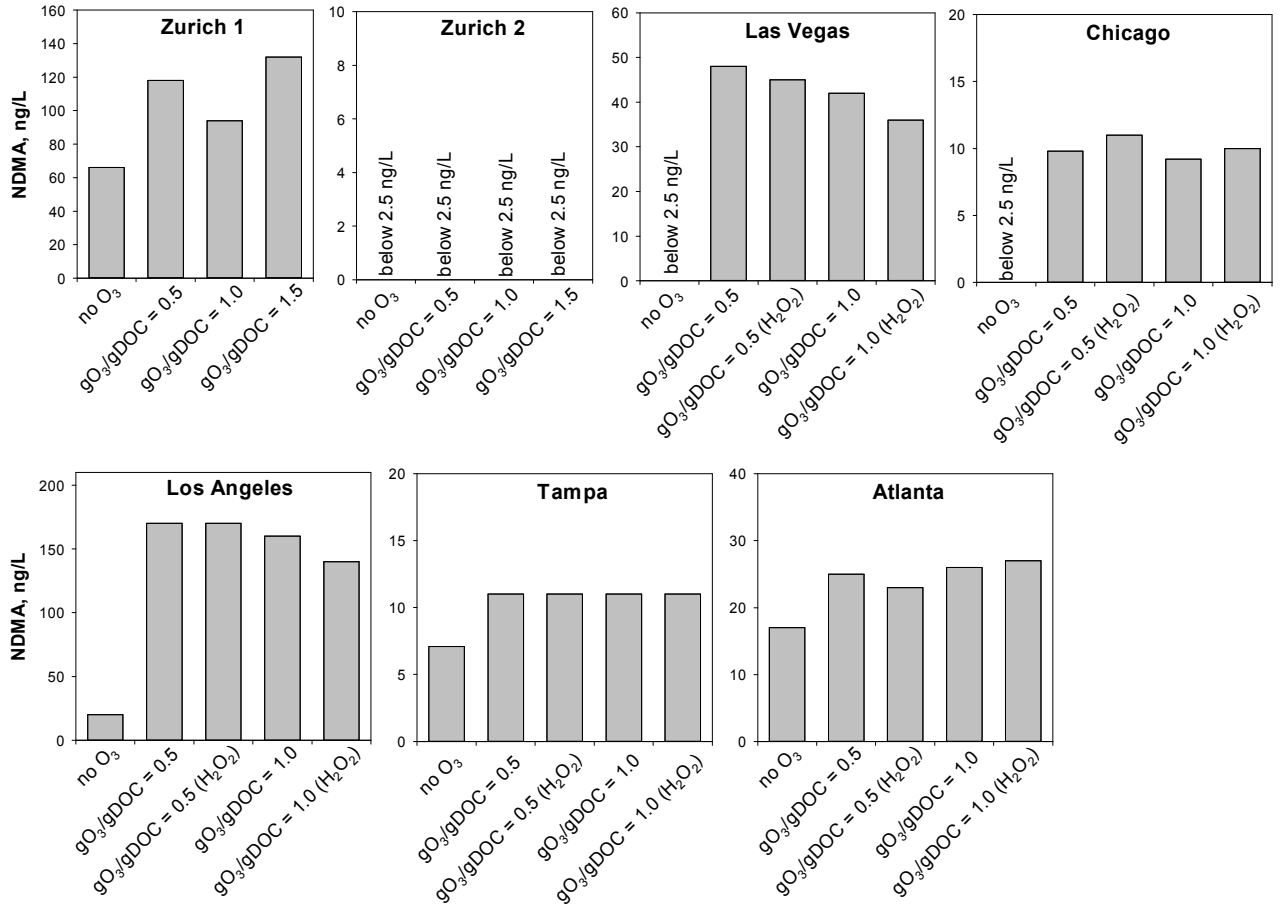

Figure S12. NDMA concentration before (no O_3) and after treatment of the selected wastewater effluents with conventional ozonation (specific ozone dose of 0.5 and 1.0 $gO_3/gDOC$) and O_3/H_2O_2 (molar ratio H_2O_2/O_3 of 0.5, indicated as (H_2O_2)). The NDMA concentration below the quantification limit of the analytical method (i.e., 2.5 ng/L), it is indicated as 'below 2.5 ng/L'.

References

(1) Bader, H.; Sturzenegger, V.; Hoigné, J. Photometric method for the determination of low concentrations of hydrogen peroxide by the peroxidase catalyzed oxidation of *N*,*N*-diethyl-p-phenylendiamine (DPD). *Water Res*. **1988**, *22*, 1109-1115.

(2) Snyder, S.A.; von Gunten, U.; Amy, G.; Debroux, J. *Use of Ozone in Water Reclamation for Contaminant Oxidation, Final Project Report and User Guidance*, WateReuse Research Foundation: Alexandria, VA, 2012

(3) Lee, Y.; Gerrity, D.; Lee, M.; Bogeat, A.E.; Salhi, E.; Gamage, S.; Trenholm, R.A.; Wert, E.C.; Snyder, S.A.; von Gunten, U. Prediction of micropollutant elimination during ozonation of municipal wastewater effluents: use of kinetic and water specific information. *Environ. Sci. Technol.* **2013**, *47*, 5872−5881.

(4) Holady, J.C.; Trenholm, R.A.; Snyder, S.A. Analysis of NDMA and other nitrosamines in water using automated solid phase extraction and gas chromatography-tandem mass spectrometry. *American Laboratory* **2012**, *44*, 25−30.

(5) Gerrity, D.; Pisarenko, A.N.; Marti, E.; Trenholm, R.A.; Gerringer, F.; Reungoat, J.; Dickenson, E. Nitrosamines in pilot-scale and full-scale wastewater treatment plants with ozonation. *Water Res.* **2015,** *72*, 251−261.

(6) Vanderford, B.J.; Snyder, S.A. Analysis of pharmaceuticals in water by isotope dilution liquid chromatography/tandem mass spectrometry. *Environ. Sci. Technol.* **2006**, *40,* 7312−7320.

(7) Huber, S.A.; Balz, A.; Abert, M.; Pronk, W. Characterization of aquatic humic and non-humic matter with size-exclusion chromatography-organic carbon detection-organic nitrogen detection (LC-OCD-OND). *Water Res.* **2011**, *45*, 879−885.

(8) Gerrity, D.; Gamage, S.; Jones, D.; Korshin, G.V.; Lee, Y.; Pisarenko, A.; Trenholm, R.A.; von Gunten, U.; Wert, E.C.; Snyder, S.A. Development of surrogate correlation models to predict trace organic contaminant oxidation and microbial inactivation during ozonation. *Water Res.* **2012**, *46*, 6257−6272.

(9) Bolton, J.R.; Linden, K.G. Standardization of methods for fluence (UV dose) determination in bench-scale UV experiments. *J. Environ. Eng.* **2003**, *129*, 209−215.

(10) Kuo, J.; Chen, C.; Nellor, M. Standardized collimated beam testing protocol for water/wastewater ultraviolet disinfection. *J. Environ. Eng*. **2003**, *129*, 774–779.

(11) Canonica, S.; Meunier, L.; von Gunten, U. Photodegradation of selected pharmaceuticals during UV treatment of drinking water. *Water Res.* **2008**, *42*, 121−128.

(12) Baxendale, J.H.; Wilson, J.A. The photolysis of hydrogen peroxide at high light intensities. *Trans. Faraday Soc*. **1957**, *53*, 344−356.

(13) Bolton, J.R.; Stefan, M.I. Fundamental photochemical approach to the concepts of fluence (UV dose) and electrical energy efficiency in photochemical degradation reactions. *Res. Chem. Intermed.* **2002**, *28*, 857−870.

(14) Wols, B.A.; Hofman-Caris, C.H.M. Review of photochemical reaction constants of organic micropollutants required for UV advanced oxidation processes in water. *Water Res.* **2002**, *46*, 2815−2827.

(15) Glaze, W. H.; Lay, Y.; Kang, J. W. Advanced oxidation processes- a kinetic-model for the oxidation of 1,2-dibromo-3-chloropropane in water by the combination of hydrogen-peroxide and UV-radiation. *Ind. Eng. Chem. Res.* **1995**, *34*, 2314–2323.

(16) Lee, Y.; von Gunten, U. Oxidative transformation of micropollutants during municipal wastewater treatment: Comparison of kinetic aspects of selective (chlorine, chlorine dioxide, ferrateVI, and ozone) and non-selective oxidants (hydroxyl radical). *Water Res*. **2010**, *44*, 555−566.

(17) von Gunten, U.; Oliveras, Y. Advanced oxidation of bromide-containing waters: bromate formation mechanisms. *Environ. Sci. Technol*. **1998,** *32*, 63-70.

(18) Pinkernell, U.; von Gunten, U. Bromate minimization during ozonation: mechanistic considerations. *Environ. Sci. Technol*. **2001,** *35*, 2525-2531.

(19) Mack, J.; Bolotn, J.R. Photochemistry of nitrite and nitrate in aqueous solution: a review. *J. Photochem. Photobiol. A: Chem.* **1999,** *128*, 1-13.

(20) NDRL/NIST Solution Kinetics Database, available at http://kinetics.nist.gov/solution/

(21) Wildhaber, Y.S.; Mestankova, H.; Schärer, M.; Schirmer, K.; Salhi, E.; von Gunten, U. Novel test procedure to evaluate the treatability of wastewater with ozone. *Water Res.* **2015,** *75*, 324–335.

(22) Katsoyiannis, I.A.; Canonica, S.; von Gunten, U. Efficiency and energy requirements for the transformation of organic micropollutants by ozone, ozone/H_2O_2 and UV/H_2O_2. **2011**, *45*, 3811–3822.

(23) Lekkerkerker-Teunissen, K.; Knol, A.H.; van Altena, L.P.; Houtman, C.J.; Verberk, J.Q.J.C.; van Dijk, J.C. Serial ozone/peroxide/low pressure UV treatment for synergistic and effective organic micropollutant conversion. *Sep. Purif. Technol.* **2012**, *100*, 22–29.

(24) Baeza, C.; Knappe, D.R.U. Transformation kinetics of biochemically active compounds in low-pressure UV photolysis and UV/H_2O_2 advanced oxidation processes. *Water Res*. **2011**, *45*, 4531-4543.

(25) Meite, L.; Szabo, R.; Mazellier, P.; De Laat, J. Kinetics of phototransformation of emerging contaminants in aqueous solution. *Revue des Sciences de l'Eau* **2010**, *23*, 31-39.

(26) Huber, M.M.; Canonica, S.; Park, G.Y.; von Gunten, U. Oxidation of pharmaceuticals during ozonation and advanced oxidation processes. *Environ. Sci. Technol*. **2003,** *37*, 1016-1024.

(27) Lee, C.; Choi, W.; Yoon, Y. UV photolytic mechanism of *N*-nitrosodimethylamine in water: Roles of dissolved oxygen and solution pH. *Environ. Sci. Technol.* **2005**, *39*, 9702–9709.

(28) Sharpless, C.; Linden, K. Experimental and model comparisons of low- and medium-pressure Hg lamps for the direct and H_2O_2 assisted UV photodegradation of N-nitrosodimethylamine in simulated drinking water. *Environ. Sci. Technol*. **2003,** *37*, 1933-1940.

(29) Ho, T.-F.; Bolton, J.; Lipczynska-Kochany, E. Quantum yields for the photodegradation of pollutants in dilute aqueous solution: phenol, 4-chlorophenol and N-nitrosodimethylamine. *J. Advanced Oxid. Technol*. **1996**, *1*, 170-178.

(30) Lee, C.; Yoon, J.; von Gunten, U. Oxidative degradation of *N*-nitrosodimethylamine by conventional ozonation and the advanced oxidation process ozone/hydrogen peroxide. *Water Res.* **2007**, *41*, 581–590.

(31) Wink, D.A.; Nims, R.W.; Desrosiers, M.F.; Ford, P.C.; Keefer, L.K. A kinetic investigation of intermediates formed during the Fenton reagent mediated degradation of *N*-nitrosodimethylamine: evidence for an oxidative pathway not involving hydroxyl radical. *Chem. Res. Toxicol.* **1991**, *4*, 510−512.

(32) Mezyk, S.P.; Cooper, W.J. Madden, K.P.; Bartels, D.M. Free radical destruction of *N*-nitrosodimethylamine in water. *Environ. Sci. Technol*. **2004,** *38*, 3161-3167.

(33) Wong-Wah-Chung, P.; Rafqah, S.; Voyard, G.; Sarakha, M. Photochemical behaviour of triclosan in aqueous solutions: kinetic and analytical studies. *J. Photochem. Photobiol. A. Chem.* **2007,** *191*, 201-208.

(34) Lee and von Gunten, U. Quantitative structure-activity relationships (QSARs) for the transformation of organic micropollutants during oxidative water treatment. *Water Res.* **2012**, *46*, 6177−6195.

(35) Latch, D.E.; Packer, J.L.; Stender, B.L.; Vanoverbeke, J.; Arnold, W.A.; McNeill, K. Aqeuous photochemistry of triclosan: formation of 2,4-dichlorophenol, 2,8-dichlorobibenzo-p-dioxin, and oligomerization products. Environ. Toxicol. Chem. . **2005**, *24*, 517−525.

(36) Azrague, K.; Osterhus, S.W. Persistent organic pollutants (POPs) degradation in natural waters using a V-UV/UV/TiO_2 reactor. *Water Sci. Technol*. **2009,** *9*, 653-660.

(37) Mezyk, S.P.; Neubauer, T.J.; Cooper, W.J.; Peller, J.R. Free-radical-induced oxidative and reductive degradation of sulfa drugs in water: absolute kinetics and efficiencies of hydroxyl radical and hydrated electron reactions. *J. Phys. Chem. A*. **2007,** *111*, 9019-9024.

(38) Yuan, F.; Hu, C.; Hu, X.; Qu, J.; Yang, M. Degradation of selected pharmaceuticals in aqueous solution with UV and UV/H_2O_2. *Water Res.* **2009**, *43*, 1766−1774.

(39) Nick, K.; Schoeler, H.; Mark, G.; Soylemez, T.; Akhlaq, M.; Schuchmann, H.-P.; von Sonntag, C. Degradation of some triazine herbicides by UV radiation such as used in the UV disinfection of drinking water. *J. Water Suppl. Res. Technol. Aqua* **1992,** *41*, 82-87.

(40) Sanches, S.; Crespo, M.T.B.; Pereira, V.J. Drinking water treatment of priority pesticides using low pressure UV photolysis and advanced oxidation processes. *Water Res.* **2010**, *44*, 1809−1818.

(41) De Laat, J.; Chramosta, N.; Dore, M.; Suty, H.; Pouillot, M. Rate constants for reaction of hydroxyl radicals with some degradation by-products of atrazine by O_3 or O_3/H_2O_2. *Environ. Technol*. **1994**, 15, 419-428.

(42) Acero, J.L.; Stemmler, K. von Gunten, U. Degradation kinetics of atrazine and its degradation products with ozone and hydroxyl radicals: a predictive tool for drinking water treatment. *Environ. Sci. Technol*. **2000,** *34*, 591-597.

(43) Benitez, F.J.; Real, F.J.; Acero, J.L.; Roldan, G. Removal of selected pharmaceuticals in waters by photochemical processes. *J. Chem. Technol. Biotechnol*. **2009**, *84*, 1186-1195.

(44) Pereira, V.J.; Weinberg, H.S.; Linden, K.G.; Singer, P.C. UV degradation kinetics and modeling of pharmaceutical compounds in laboratory grade and surface water via direct and indirect photolysis at 254 nm. *Environ. Sci. Technol*. **2007,** *41*, 1682-1688.

(45) Marotta, R.; Spasiano, D.; Somma, I.D.; Andreozzi, R. Photodegradation of naproxen and its photoproducts in aqueous solution at 254 nm: A kinetic investigation. *Water Res.* **2013**, *47*, 373−383.

(46) Packer, J.L.; Werner, J.J.; Latch, D.E.; McNeill, K.; Arnold, W.A. Photochemical fate of pharmaceuticals in the environment: naproxen, diclofenac, clofibric acid, and ibuprofen. *Aquatic Science* **2003**, *65*, 342-351.

(47) Rosenfeldt, E.J.; Linden, K.G. Degradation of endocrine disrupting chemicals bisphenol-A, ethinylestradiol, and estradiol during UV photolysis and advanced oxidation processes. *Environ. Sci. Technol*. **2004,** *38*, 5476-5483.

(48) Lam, M.W.; Mabury, S.A. Photodegradation of the pharmaceuticals atorvastatin, carbamazepine, levofloxacin, and sulfamethoxazole in natural waters. *Aquatic Science* **2005**, *67*, 177-188.

(49) Real, F.J.; Benitez, F.J.; Acero, J.L.; Sagasti, J.J.P.; Casas, F. Kinetics of the chemical oxidation of the pharmaceuticals primidone, ketoprofen, and diatrizoate in ultrapure and natural waters. *Ind. Eng. Chem. Res*. **2009**, *48*, 3380-3388.

(50) Benner, J.; Salhi, E.; Ternes, T.; von Gunten, U. Ozonation of reverse osmosis concentrate: kinetics and efficiency of beta blocker oxidation. *Water Res*. **2008**, *42*, 3003-3012.

(51) Dodd, M.C.; Buffle, M.O.; von Gunten, U. Oxidation of antibacterial molecules by aqueous ozone: moiety-specific reaction kinetics and application to ozone-based wastewater treatment. *Environ. Sci. Technol*. **2006,** *40*, 1969-1977.

(52) Razavi, B.; Song, W.; Cooper, W.J. Greaves, J. Jeong, J. Free-radical-induced oxidative and reductive degradation of fibrate pharmaceuticals: kinetic studies and degradation mechanisms. *J. Phys. Chem. A* **2009,** *113*, 1287-1294.

(53) Song, W.; Cooper, W.J.; Peake, B.M.; Mezyk, S.P.; Nickelsen, M.G.; O'Shea, K.E. Free-radical-induced oxidative and reductive degradation of N,N'-diethyl-m-toluamide (DEET): Kinetic studies and degradation pathway. *Water Res.* **2009**, *43*, 635–642.